CHAPTER V

RESULTS AND DISCUSSION

The results and discussion in this chapter are divided into two major parts. In the first part, several characterization results for the catalysts are described. And the results for photocatalytic degradation of crocein orange G and methylene blue using TiO_2 as the photocatalyst in an airlift reactor are discussed in the last section.

5.1 Characterization of catalyst

5.1.1 Phase structure and crystallite size

In this study TiO_2 catalyst was prepared via a sol-gel method and was calcined at 200 °C for one hour. The bulk crystalline phases of TiO_2 catalyst were determined using X-ray dtffractometry (XRD). XRD result of TiO_2 sample was displayed in Figure 5.1

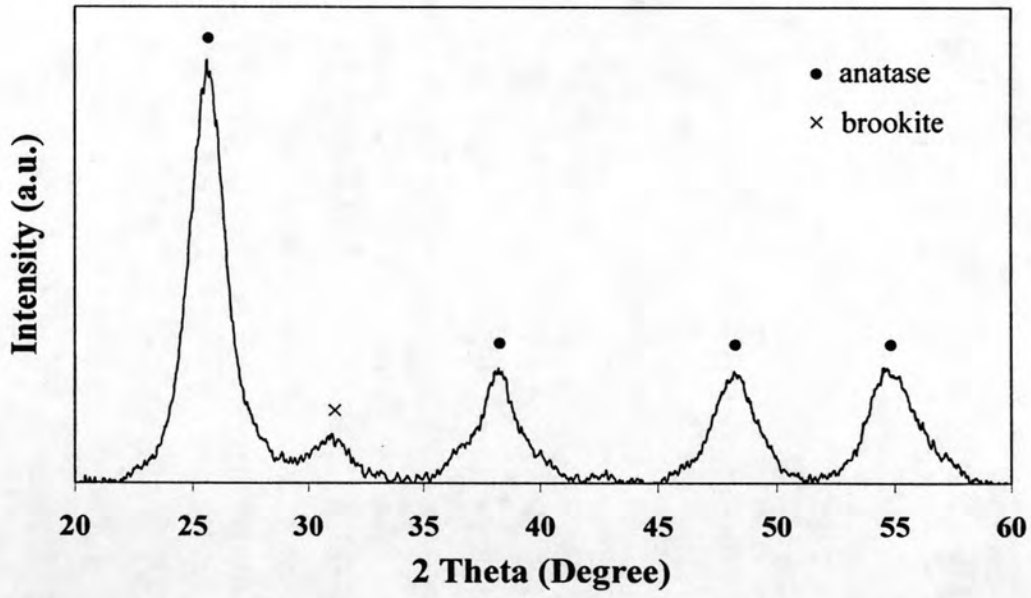

Figure 5.1 XRD patterns of titania calcined at 200 °C for one hour.

From the XRD patterns of TiO_2, the dominant peaks of anatase were observed at 2θ of about 25.2°, 37.9°, 47.8°, and 53.8°, which represent the indices of (101), (004), (200), and (105) planes, respectively. The weak peak at about 2θ = 30.86° was assigned to brookite phase of TiO_2 and XRD peaks that belong to rutile phase were not detected at this temperature. Therefore, TiO_2 catalyst primarily consists of anatase phase. The average crystallite size was calculated from Scherer's equation using the broadening of (101) diffraction peak in XRD pattern. The crystallite size of anatase was approximately 4.9 nm.

5.1.2 Measurement of specific surface area

Specific surface area of TiO_2 that was calcined at 200 °C for one hour was determined by nitrogen physisorption technique using Brunauer – Emmett – Taylor isotherm. The sample possessed reasonably high specific surface area of 170 $m^2 g^{-1}$.

5.2 Photocatalytic degradation of organic dyes

5.2.1 Effect of the ratio between the downcomer and riser cross sectional area (A_d/A_r) on the photocatalytic degradation of crocein orange G

In this section, the effect of design configuration in the airlift system on its performance was investigated. A basic design parameter in the airlift system is the ratio between cross sectional areas of downcomer and riser (A_d/A_r), which could be simply altered by changing the draft tube size. The two diameters of draft tube employed were 4.6 and 6.6 cm, which gave A_d/A_r of approximately 3.0 and 0.9, respectively. Crocein orange G was employed in this experiment. The experiment was divided into two parts, adsorption and photocatalytic degradation, as mention in Section 4.4.3. The conditions employed for this study were an initial concentration of 5 ppm, an aeration rate of 12 l/min, and no pH adjustment.

Figure 5.2 shows the results from the adsorption experiment, where C was the concentration of dye after irradiation time t of the photocatalytic degradation, C_0 is the initial concentration of dye. There was almost no effect of the area ratio on the

adsorption rate of crocein orange G. An increase in the downcomer to riser cross-sectional area ratio (A_d/A_r) increased the liquid circulation velocity in the airlift reactor (Al-Masry and Abasaeed, 1998). This implied that there was no mass transfer limitation in the adsorption process of crocein orange G.

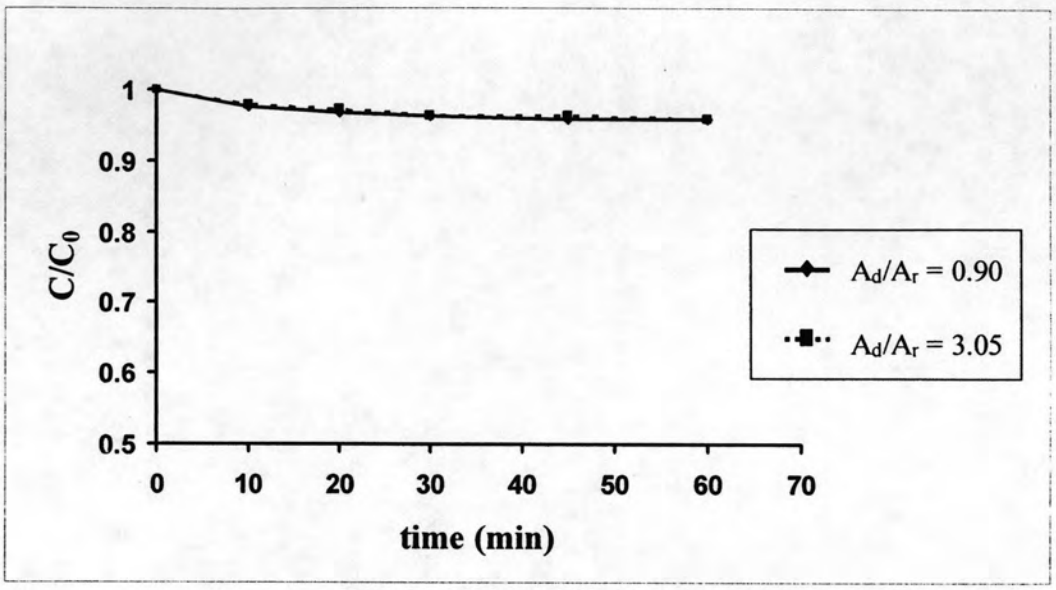

Figure 5.2 Effect of A_d/A_r ratios on adsorption rate of crocein orange G on TiO_2 in an airlift reactor system (condition: C_0 = 5 ppm, Aeration rate = 12 l/min, pH = 5.57).

Figure 5.3 displays the results for the photocatalytic degradation of crocein orange G in an airlift reactor system with two A_d/A_r ratios. Similarly, there was no significant effect of this parameter on the photocatalytic degradation of crocein orange G.

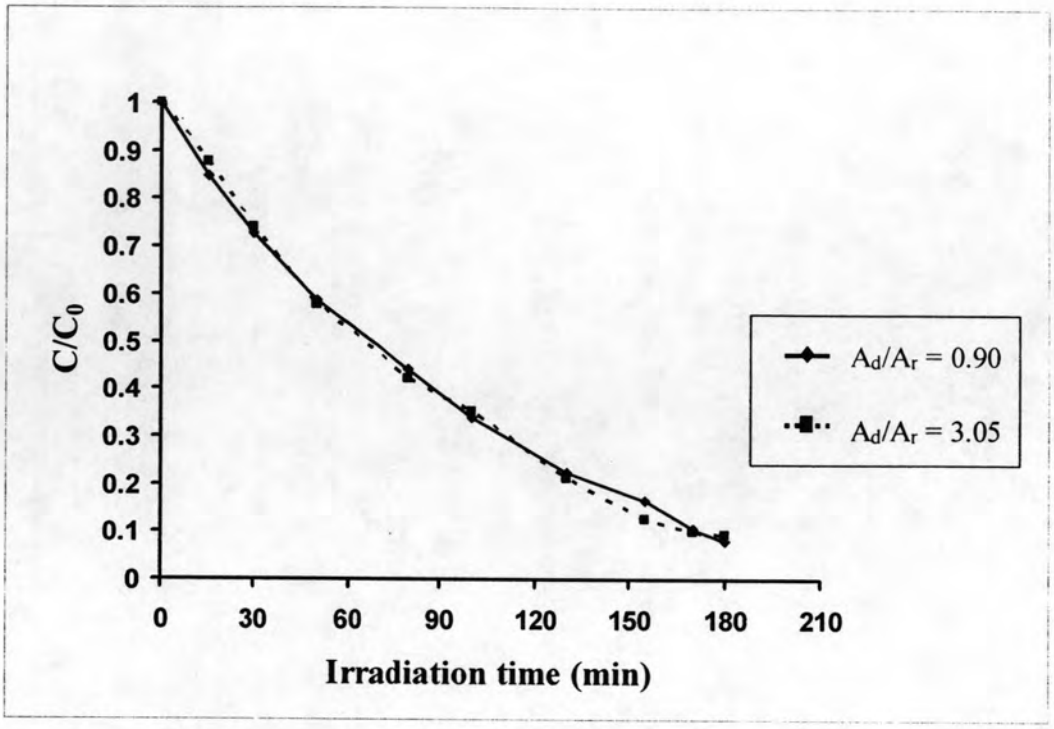

Figure 5.3 Effect of A_d/A_r ratios on photocatalytic degradation of crocein orange G over TiO_2 in an airlift reactor system (condition: C_0 = 5 ppm, Aeration rate = 12 l/min, pH = 5.57).

To investigate these results, further dissolved oxygen concentration (DOC) and the light intensity were measured simultaneously while the photocatalytic degradation was undergoing. Figures 5.4 and 5.5 show the results for DOC and light intensity measurements, respectively. We did not observe any difference in the results when A_d/A_r ratio changed for both DOC and light intensity. These results could explain why there was no effect of A_d/A_r on the photocatalytic degradation of crocein orange G in an airlift reactor.

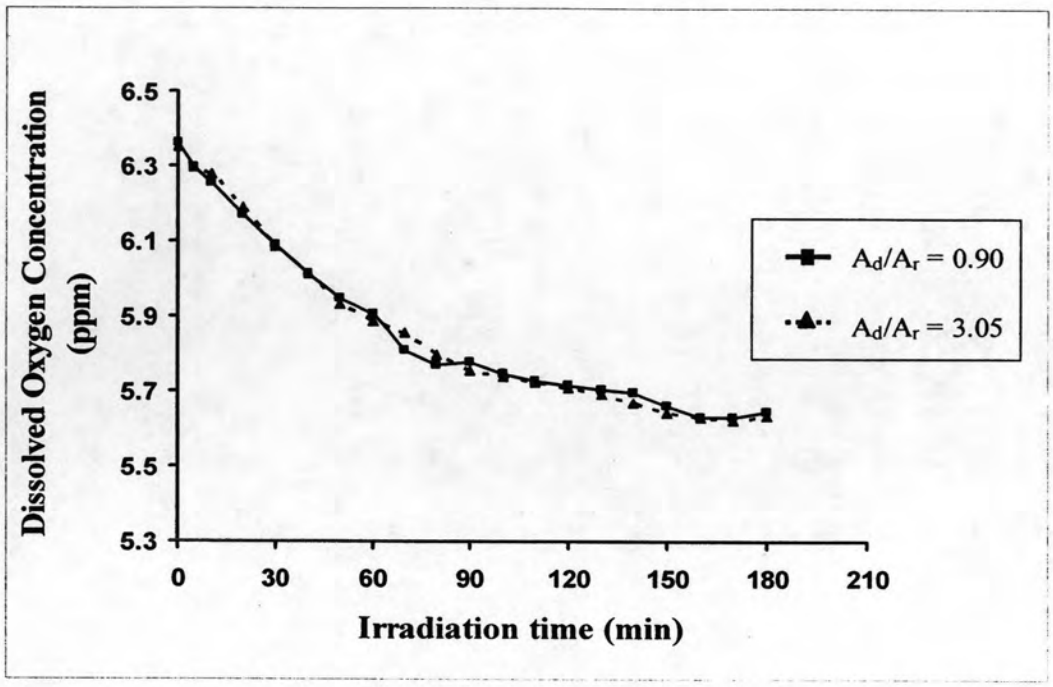

Figure 5.4 Effect of A_d/A_r ratios on dissolved oxygen concentration in the photocatalytic degradation of crocein orange G in an airlift reactor system (condition: C_0 = 5 ppm, Aeration rate = 12 l/min, pH = 5.57).

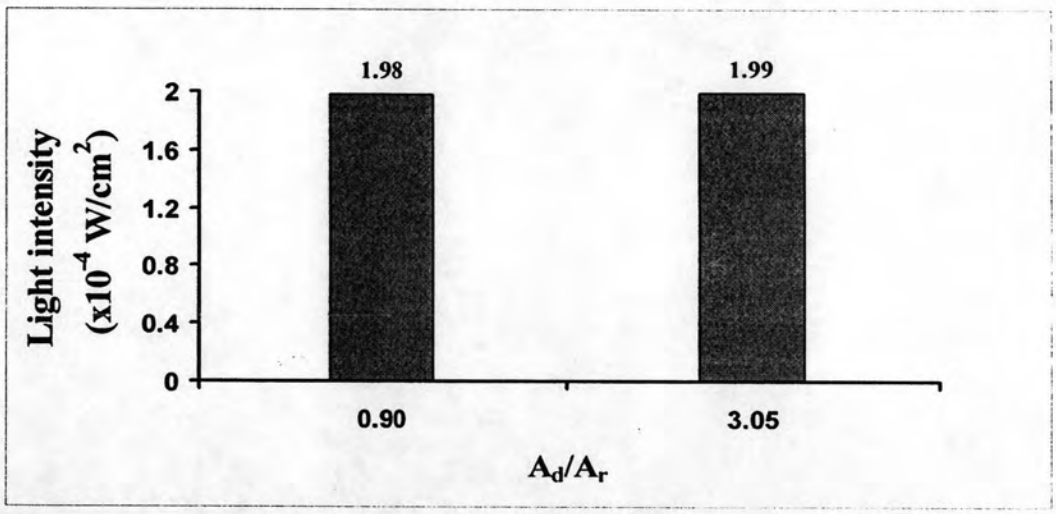

Figure 5.5 Effect of A_d/A_r ratios on the light intensity in the photocatalytic degradation of crocein orange G in an airlift reactor system (condition: C_0 = 5 ppm, Aeration rate = 12 l/min, pH = 5.57).

5.2.2 Effect of aeration rate on the photocatalytic degradation of crocein orange G

In this section, the effect of aeration rate on the photocatalytic degradation of crocein orange G in an airlift reactor system was investigated. Three aeration rates were employed, namely, 6 l/min, 9 l/min, and 12 l/min. The experiment was divided into two parts, adsorption and photocatalytic degradation. The conditions employed for this set of experiments were an initial concentrations of 15 ppm during adsorption and 5 ppm during photocatalytic degradation, and no pH adjustment.

Figure 5.6 shows the adsorption behavior of 15 ppm of crocein orange G in an airlift reactor system at different aeration rates. There was no significant impact of aeration rate on the adsorption behavior of crocein orange G. An increase in aeration rate increased the liquid circulation velocity in the airlift reactor (Al-Masry and Abasaeed, 1998). Therefore, there was no mass transfer limitation in the adsorption of crocein orange G during the experiment.

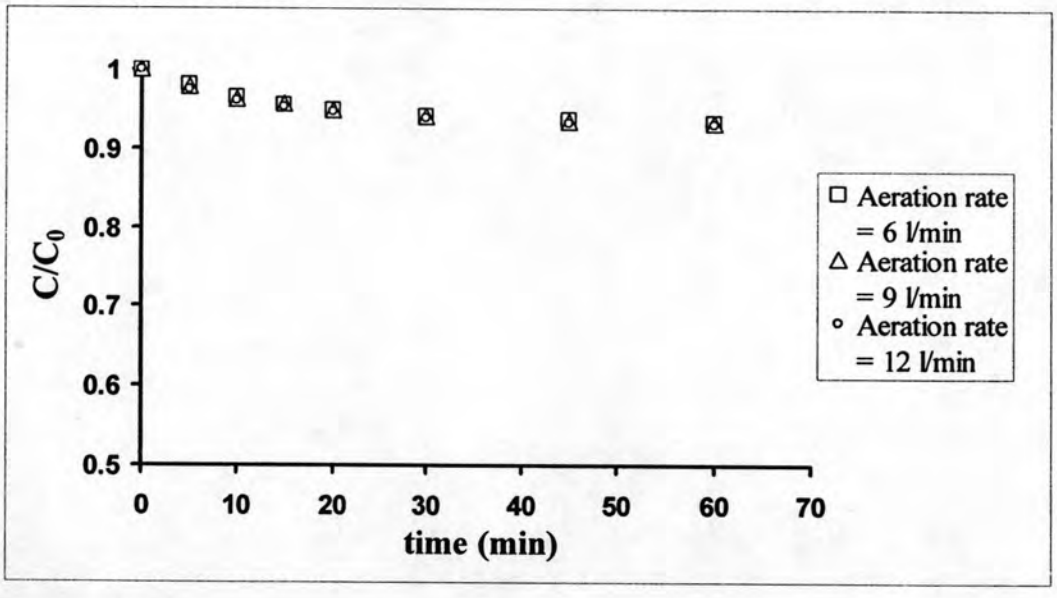

Figure 5.6 Effect of aeration rate on adsorption behavior of crocein orange G in an airlift reactor system (condition: C_0 = 15 ppm, pH = 5.57).

Figure 5.7 shows the results for photocatalytic degradation of 5 ppm of crocein orange G in an airlift reactor system at different aeration rates. As aeration rate increased, the photodegradation rate of crocein orange G became faster.

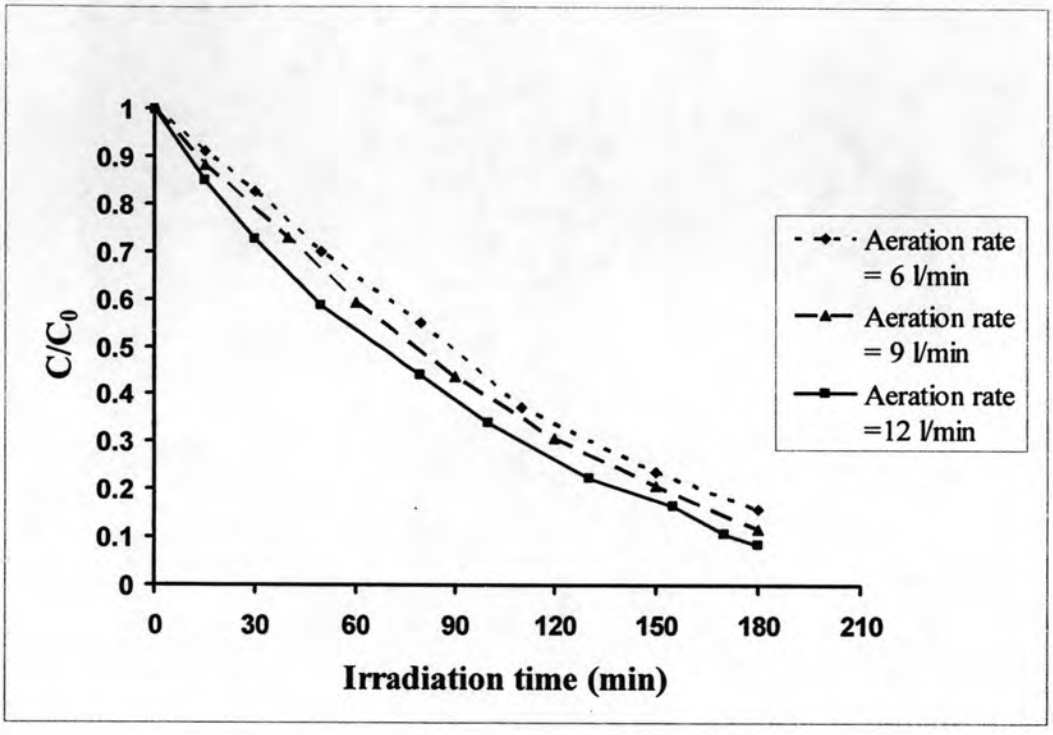

Figure 5.7 Effect of aeration rate on the photocatalytic degradation of crocein orange G in an airlift reactor system (condition: C_0 = 5 ppm, pH = 5.57).

To explain this result, we measured dissolved oxygen concentration (DOC) and light intensity inside the reactor during the experiments and the results are displayed in Figures 5.8 and 5.9. At an aeration rate of 12 l/min, the DOC was the greatest. When the aeration rate was decreased, the DOC became lower. However, the light intensity changed only slightly as aeration rate changed so its effect may be negligible.

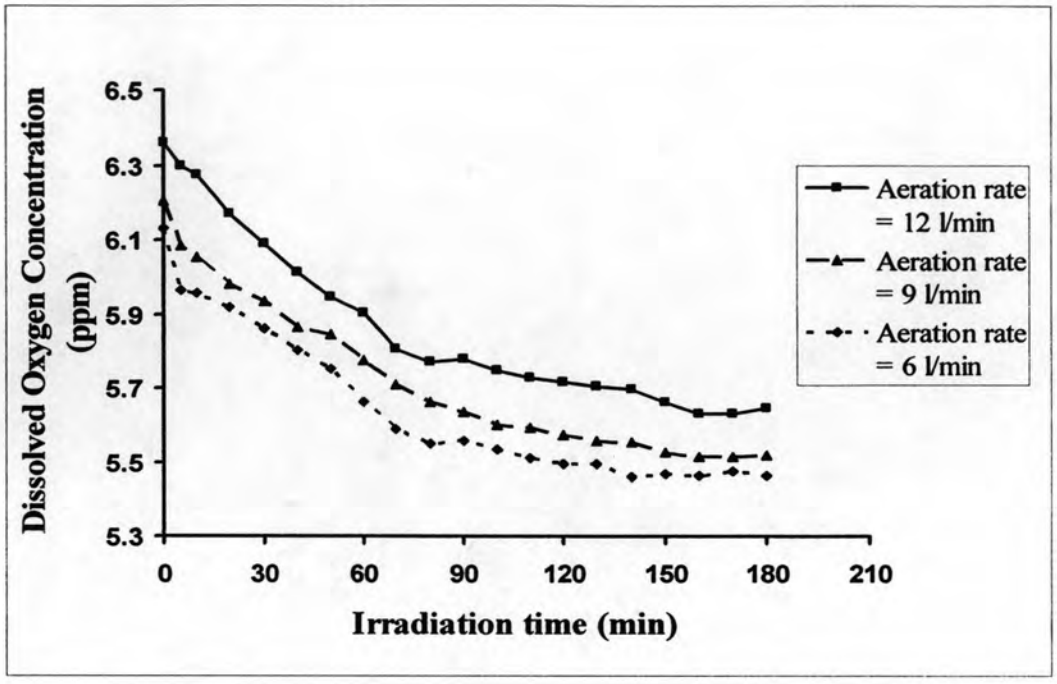

Figure 5.8 Effect of aeration rate on dissolved oxygen concentration in the photocatalytic degradation of crocein orange G in an airlift reactor system (condition: C_0 = 5 ppm, pH = 5.57).

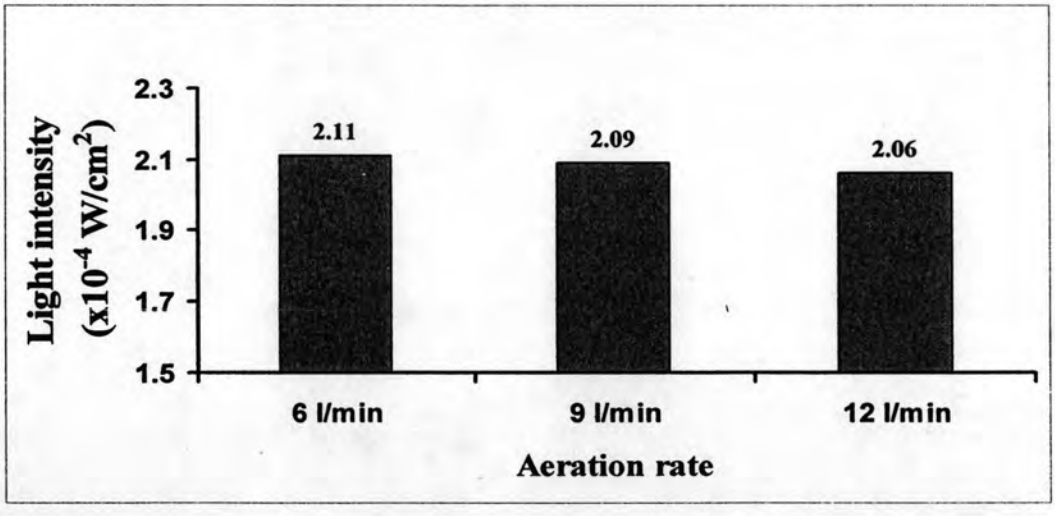

Figure 5.9 Effect of aeration rate on the light intensity in the photocatalytic degradation of crocein orange G in an airlift reactor system (condition: C_0 = 5 ppm, pH = 5.57).

An increase in the aeration rate increased the supply of oxygen by means of enhanced turbulence, gas holdup, gas–liquid interfacial area, and greater mass transfer coefficient. The dissolved oxygen was a result of air bubbling through the liquid on the surface of TiO_2, which prevented the recombination process by trapping electrons generated by UV irradiation. The positive influence of oxygen concentration in photocatalytic system can be attributed to enhancing the separation of photogenerated electron-hole pairs, hereby increasing hydroxyl and superoxide radical concentration. Hence, the degree of photodegradation increased with an increase in the aeration rate. Also, possible breakage of the particles because of attrition at a larger airflow rate may generate a larger catalyst surface area, thereby, increasing the rate of degradation [Chakrabarti et al, 2004; Daneshvar et al, 2004]

5.2.3 Effect of pH

In this section, the effect of pH of the dye solution on the photocatalytic degradation of dye in an airlift reactor system was investigated. Crocein orange G and methylene blue were employed in this study. The experiment was divided into two parts, adsorption and photocatalytic degradation.

5.2.3.1 Effect of pH on the photocatalytic degradation of crocein orange G

In order to study the effect pH on the adsorption of crocein orange G on TiO_2, a series of experiments was conducted at pH values of 2.0, 4.0, 5.57 (natural pH), and 8.0. The suspension was stirred in the dark for 60 min during adsorption period. The initial concentration of crocein orange G was 5 ppm and the aeration rate was 12 l/min.

The adsorption behaviors for crocein orange G at various pH are presented in Figure 5.10. As pH decreased from 8.0 to 2.0, more crocein orange G was adsorbed on TiO_2.

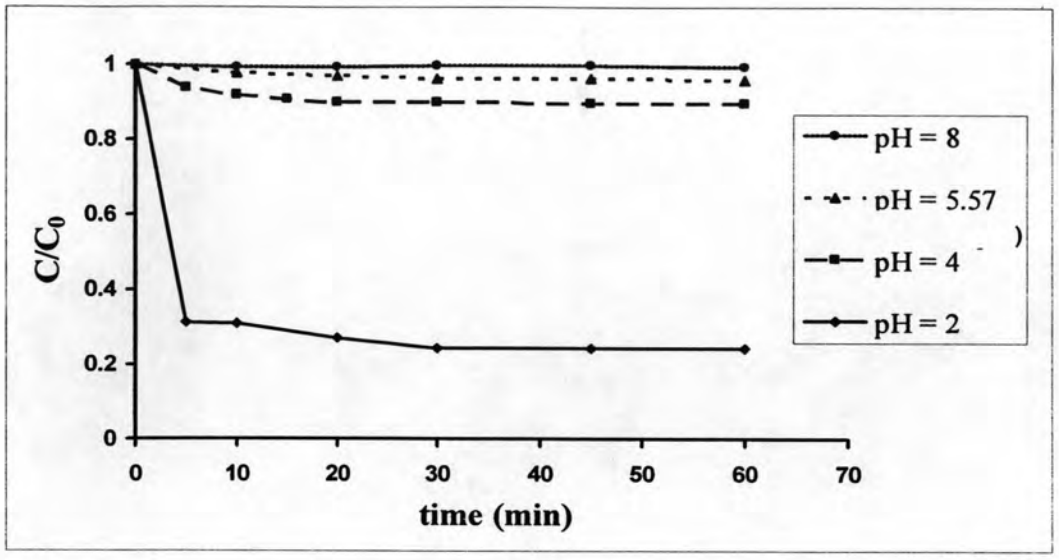

Figure 5.10 Effect of pH on the adsorption behavior of crocein orange G on TiO_2 in an airlift reactor system (condition: C_0 = 5 ppm, aeration rate = 12 l/min).

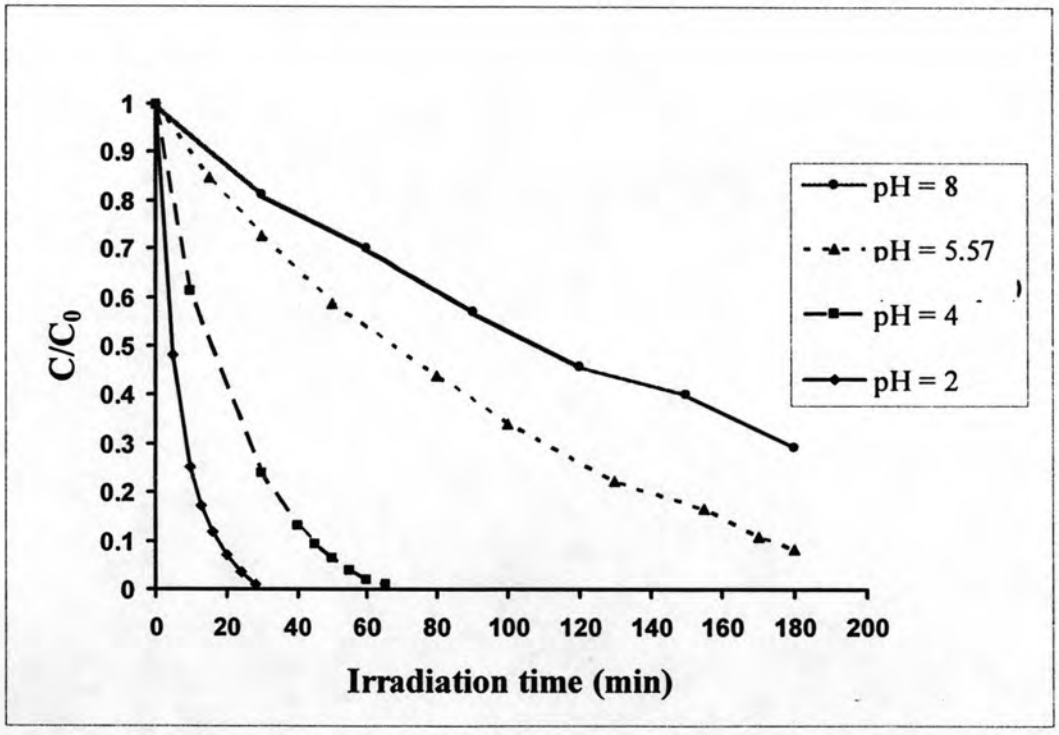

Figure 5.11 Effect of pH on the photocatalytic degradation of crocein orange G in an airlift reactor system (condition: C_0 = 5 ppm, aeration rate = 12 l/min).

The kinetic of photocatalytic degradation of crocein orange G at various pH are presented in Figure 5.11. As the pH of the solution decreased from 8.0 to 2.0, the rate of photocatalytic degradation of crocein orange G became faster. Since the photocatalytic degradation of crocein orange G were performed after 60 minutes allocated for adsorption, the initial concentration for the photocatalytic degradation at each pH differed from one another. Nevertheless, when we considered the overall performance of the system, photocatalytic degradation of crocein orange G was the most effective at acidic pH of 2.

The explanation of these results concerns the influence of pH on both the surface state of titania and the ionization state of ionizable organic molecules. At a pH above the point of zero charge (pzc) of titania (titania synthesized by sol-gel method has the pzc of 4), the surface of titania became negatively charged. In contrary, the surface of titania was positively charged at a pH below the pzc, according to the following equilibria:

$$pH < pzc : Ti\text{-}OH + H^+ \Leftrightarrow TiOH_2^+ \qquad (5.1)$$

$$pH > pzc : Ti\text{-}OH + OH^- \Leftrightarrow TiO^- + H_2O \qquad (5.2)$$

Since crocein orange G is an anionic dye and contains the negatively charged sulfonate SO_3^- group. In acidic solution, TiO_2 had positive charge on the surface. As a result, an electrostatic attraction between the positive TiO_2 surface and an anionic dye led to strong adsorption and eventually high rate of degradation. On the other hand, in basic solution, an electrostatic repulsion between the negatively charged surface of TiO_2 and an anionic dye led to weak adsorption and retarded the degradation rate of the dye.

This finding about the influence of pH on the photocatalytic degradation of crocein orange G agreed with previous works done by other groups by several past reports. Sun and coworkers [2006] stated that the pH value of crocein orange G solution had significant influence on the photocatalytic activity, which controls the production rate of hydroxyl radical. The photodegradation of crocein orange G was the most efficient in acidic solution and the optimal pH was about 2.0.

The lower the pH value, the higher the position of the valence band. Consequently, TiO_2 had higher activity in oxidating organic pollutants. At pH below 2.0 the degradation efficiency also decreased because in crocein orange G, the azo linkage (–N=N–) was particularly susceptible to electrophilic attack by hydroxyl radical. But at low pH the concentration of H^+ was in excess and H^+ ions interacted with the azo linkage reducing the electron densities at the azo group. Consequently, the reactivity of hydroxyl radical by the electrophilic mechanism decreased.

Lachheb and coworkers [2002] stated that the pH had positive influence on the kinetics of disappearance of crocein orange G. The results were represented by the form of linear transformation, according to the following equation:

$$\log k_{app} = f(\log [H^+]) = f(-pH) \qquad (5.3)$$

This representation enabled one to determine the kinetic partial order with respect to proton concentration by measuring the slopes of the curves. The results indicated that for the photocatalytic degradation of crocein orange G, an increase of the H^+ (a decrease of pH of solution) increased k_{app} of this reaction.

5.2.3.2 Effect of pH on the photocatalytic degradation of methylene blue

In order to study the effect pH on the adsorption of methylene blue on TiO_2, a series of experiments was conducted at pH values of 4, 5.37 (natural pH), 8, and 10. The suspension was stirred in the dark for 60 min during adsorption period as same as the adsorption of crocein orange G The initial concentration of methylene blue was 5 ppm and the aeration rate was 12 l/min.

The adsorption behaviors for methylene blue at various pH are presented in Figure 5.12. As pH increased from 4.0 to 10.0, more methylene blue was adsorbed on TiO_2.

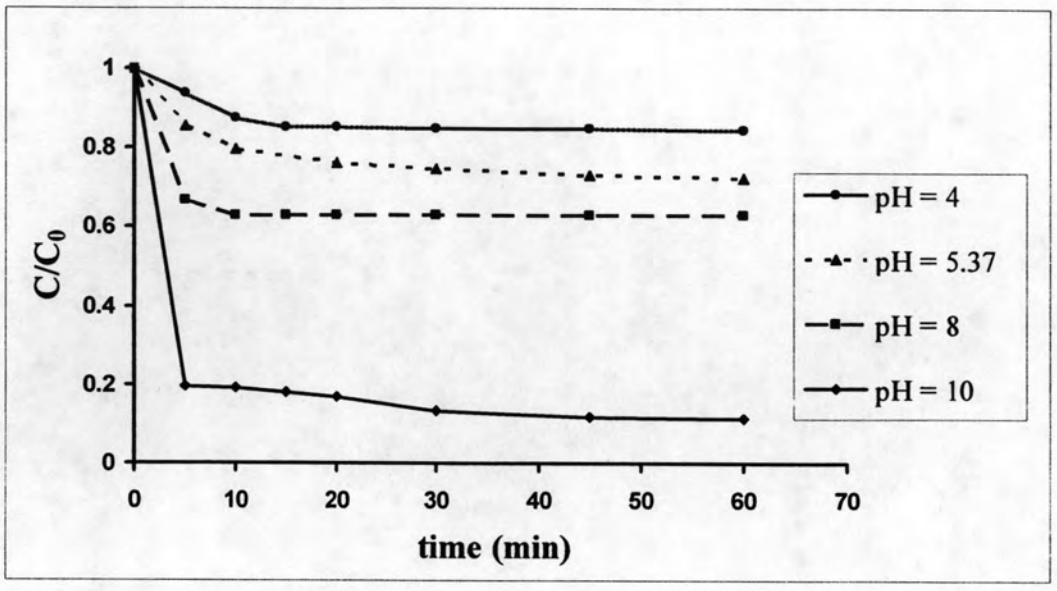

Figure 5.12 Effect of pH on the adsorption behavior of methylene blue on TiO_2 in an airlift reactor system (condition: C_0 = 5 ppm, aeration rate = 12 l/min).

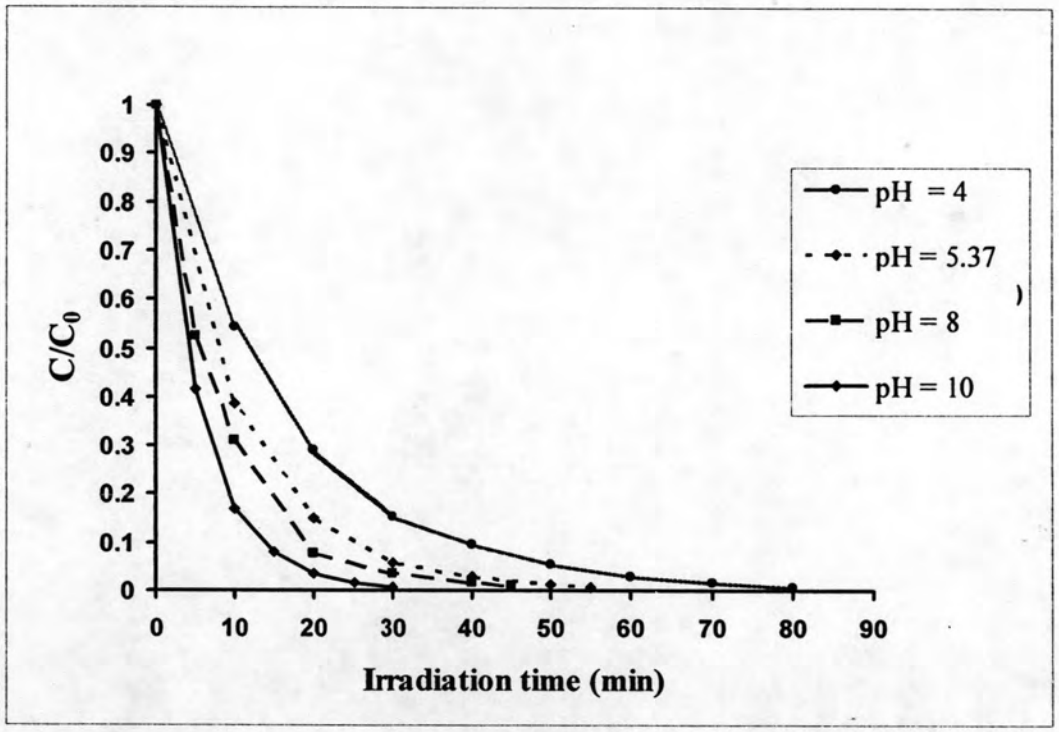

Figure 5.13 Effect of pH on the photocatalytic degradation of methylene blue in an airlift reactor system (condition: C_0 = 5 ppm, aeration rate = 12 l/min).

The kinetics of photocatalytic degradation of methylene blue at various pH were presented in Figure 5.13. An increase in the pH from 4 to 10 enhanced the performance of photocatalytic degradation of methylene blue. Similar to the photocatalytic degradation of crocein orange G, the photocatalytic degradation of methylene blue were performed after 60-minute period allocated for adsorption, the initial concentration for the photocatalytic degradation at each pH differed from one another. Nevertheless, when we considered the overall performance of the system, photocatalytic degradation of methylene blue was the most effective at basic pH of 10.

The explanation of these results were similar to the one given for crocein orange G earlier. The pH influenced both the surface state of titania and the ionization state of ionizable organic molecules. However, methylene blue is a cationic dye. At high pH, the adsorption of methylene blue was favorable on a negatively charged surface of TiO_2, leading to high rate of degradation.

This finding about the influence of pH to the photocatalytic degradation of methylene blue agreed with works by other researchers. Lachheb and coworkers [2002] explained why the pH had positive influence on the kinetics of disappearance of methylene blue with the same reason described for crocein orange G earlier. For the photocatalytic degradation of methylene blue, an increase in pH of solution increased k_{app} of the reaction.

5.2.4 Effect of initial concentration of dyes

In this section, the effect of initial concentration of dyes on their photocatalytic degradation in an airlift reactor system was investigated. Crocein orange G and methylene blue were employed in this study. The initial concentrations employed in the study were 5 ppm, 10 ppm, and 15 ppm. The experiment was divided into two parts, adsorption and photocatalytic degradation. The suspension was stirred in the dark for 60 minutes to reach adsorption equilibrium. The aeration rate was 12 l/min and the pH of the solution was not adjusted. The adsorption behavior for crocein orange G and methylene blue are presented in Figures 5.14 and 5.15, respectively.

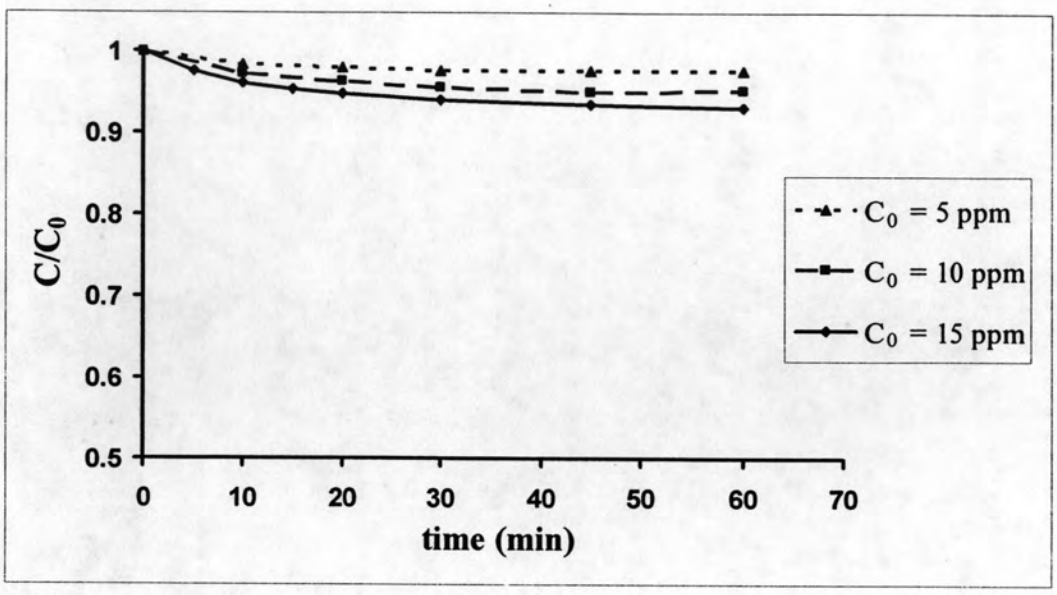

Figure 5.14 Effect of initial concentration of crocein orange G on its adsorption behavior on TiO_2 in an airlift reactor system (condition: aeration rate = 12 l/min, pH = 5.57).

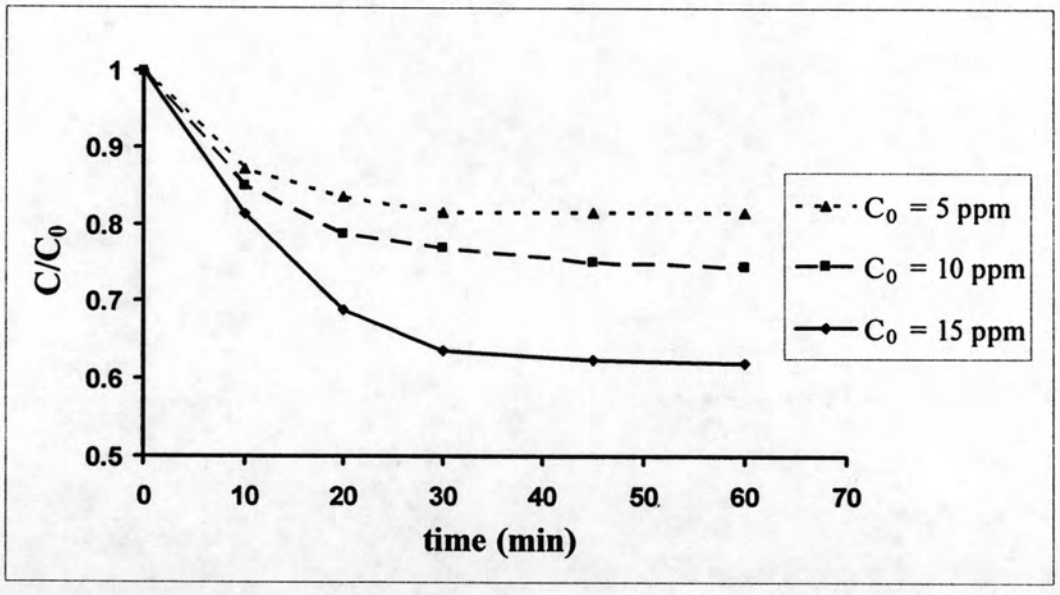

Figure 5.15 Effect of initial concentration of methylene blue on its adsorption behavior on TiO_2 in an airlift reactor system (condition: aeration rate = 12 l/min, pH = 5.37).

An increase in the initial concentration increased the adsorption for both dyes on TiO_2. Greater adsorption of methylene blue compared to that of crocein orange G could be attributed to the pH of the solution. The natural pH of solutions of methylene blue and crocein orange G were 5.37 and 5.57, respectively, both of which were above the pzc of titania. As mention earlier, the surface of TiO_2 became negatively charged above the pzc. Since crocein orange G is an anionic dye while methylene blue is a cationic dye, at natural pH condition the adsorption of methylene blue on TiO_2 was higher than that of crocein orange G.

The effect of initial concentration of dyes on their photocatalytic degradation was also investigated. The kinetics of photocatalytic degradation of crocein orange G and methylene blue are presented in Figures 5.16 and 5.17, respectively. The photocatalytic degradation of both dyes were performed continuously after the 60-minute period of adsorption.

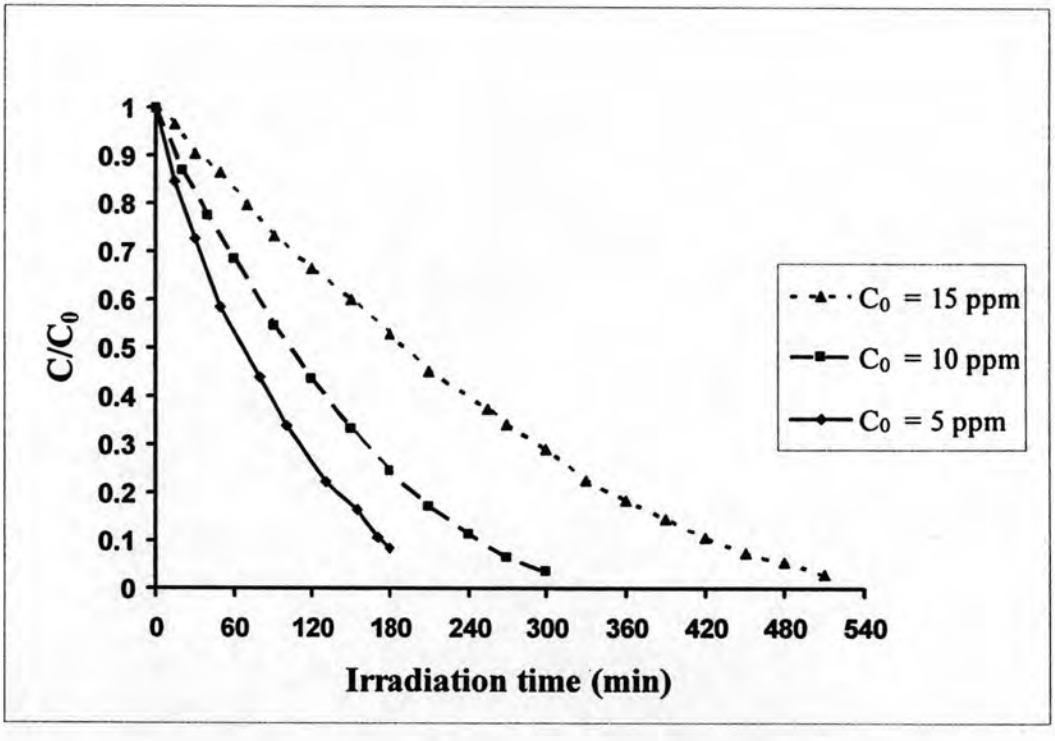

Figure 5.16 Effect of initial concentration of crocein orange G on its photocatalytic degradation in an airlift reactor system (condition: aeration rate = 12 l/min, pH = 5.57).

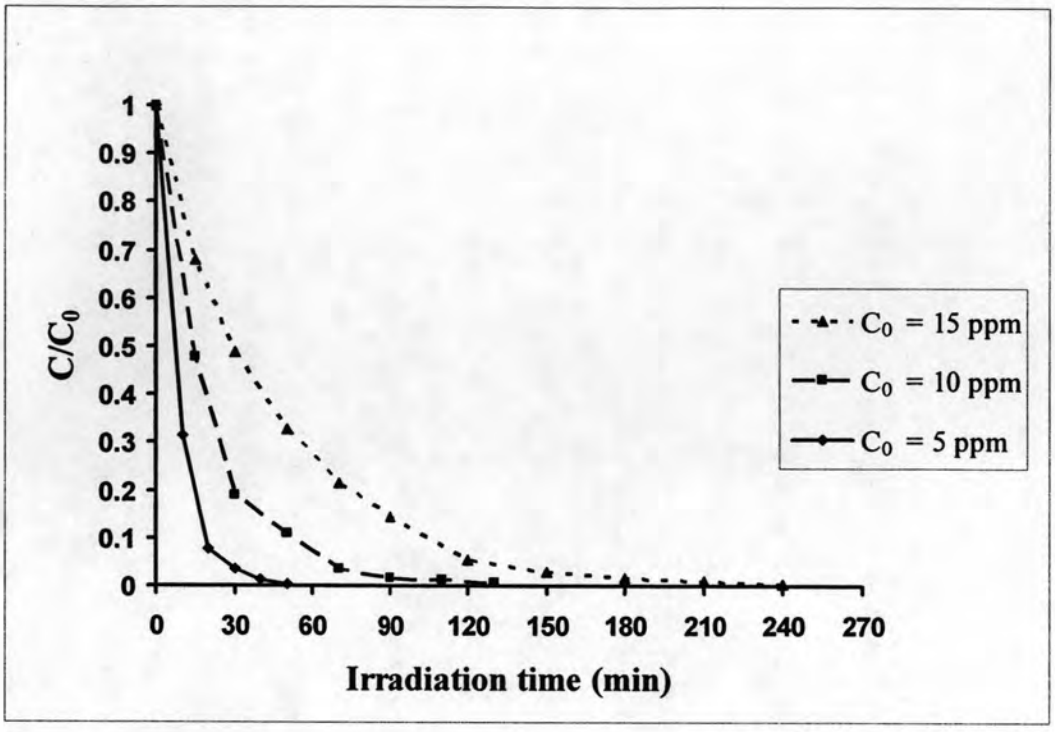

Figure 5.17 Effect of initial concentration of methylene blue on its photocatalytic degradation in an airlift reactor system (condition: aeration rate = 12 l/min, pH = 5.37).

Inspection of the figures indicated that the rates for photocatalytic degradation of both dyes were faster at lower initial concentrations. The dependence of reaction rate to initial dyes concentration could be related to the formation of several layers of adsorbed dye on the surface of titania, which was higher at higher concentration of dye. The outer layers of adsorbed dye could not react with photogenerated holes or hydroxyl radicals because there was no direct contact of photocatalyst with the dye molecules. Increasing concentration of dye also caused the dye molecules to absorb the light before the photons reached the photocatalyst surface. So at higher concentration of dye, the performance of photodegradation decreased [Lee et al., 2003]. The better performance in photocatalytic degradation of methylene blue than that of crocein orange G could be explained by the consequence of the pH of the solution which led to better adsorption of methylene blue on TiO_2 and eventually faster rate of degradation.

Furthermore, the light intensity was measured during the photocatalytic degradation experiment. The results were displayed in Figures 5.18 and 5.19.

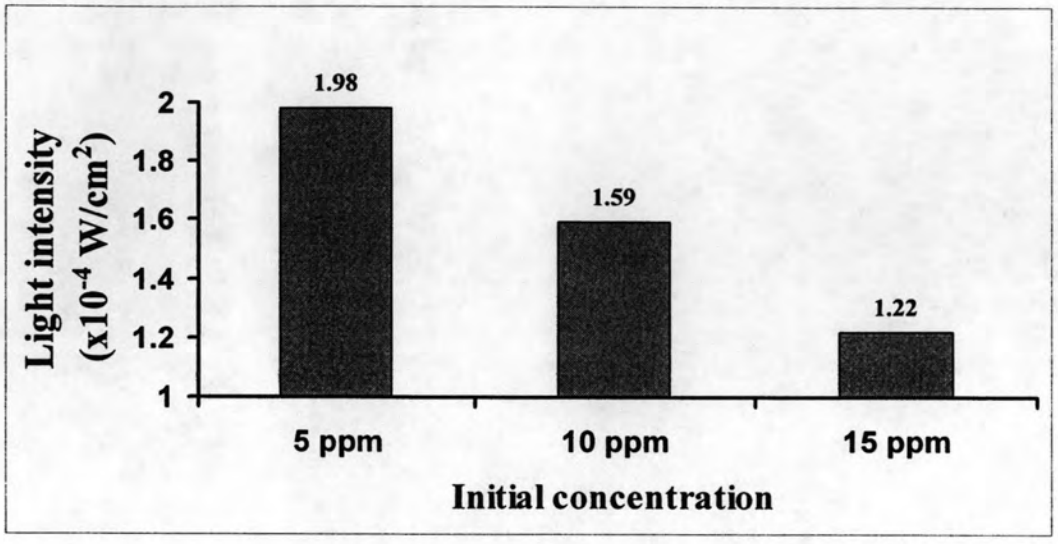

Figure 5.18 Effect of initial concentration of crocein orange G on the light intensity inside an airlift reactor (condition: aeration rate = 12 l/min, pH = 5.57).

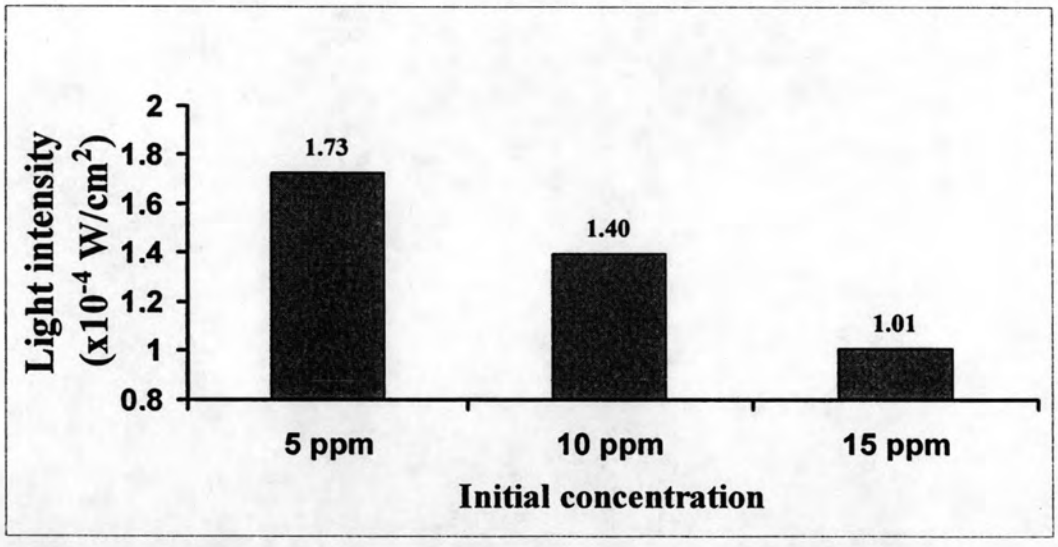

Figure 5.19 Effect of initial concentration of methylene blue on the light intensity inside an airlift reactor (condition: aeration rate = 12 l/min, pH = 5.37).

For both dyes, the light intensity decreased with increasing initial concentration of dyes. These results were in good agreement with the finding of Lee and coworker [2003] that was mentioned above. So an increase in initial concentration of dyes decreased the light intensity inside the reactor, resulting in low rate of photocatalytic degradation of such dye.

5.2.5 Photocatalytic degradation of organic dyes in various reactor systems

In this section, the photocatalytic degradation of crocein orange G and methylene blue in three different photoreactor systems were investigated, namely, airlift reactor system, bubble column reactor, and stirred tank reactor. The best experimental conditions were chosen from previous sets of experiments. The experiment was divided into two parts: adsorption and photocatalytic degradation.

5.2.5.1 Photocatalytic degradation of crocein orange G in various reactor systems

Figures 5.20 to 5.22 display the adsorption behavior of crocein orange G in three different photoreactor systems at initial concentrations of 5, 10, and 15 ppm, respectively. Different photoreactor systems appeared to have similar adsorption behavior at all values of initial concentration of dye. However, an increase in the initial concentration raised the amount of crocein orange G adsorbed on TiO_2.

After 60 minutes of adsorption without UV irradiation, the photocatalytic degradation of crocein orange G were continuously monitored. Figures 5.23 to 5.25 display the photocatalytic degradation of crocein orange G in the three photoreactor systems at various initial concentrations. Among the three photoreactor systems, airlift reactor system exhibited the best performance in the photocatalytic degradation of the dye at all initial concentrations. With an airlift reactor system, the photocatalytic degradation of crocein orange G at initial concentrations of 5, 10, and 15 ppm reached completion in 28 min, 60 min, and 90 min, respectively.

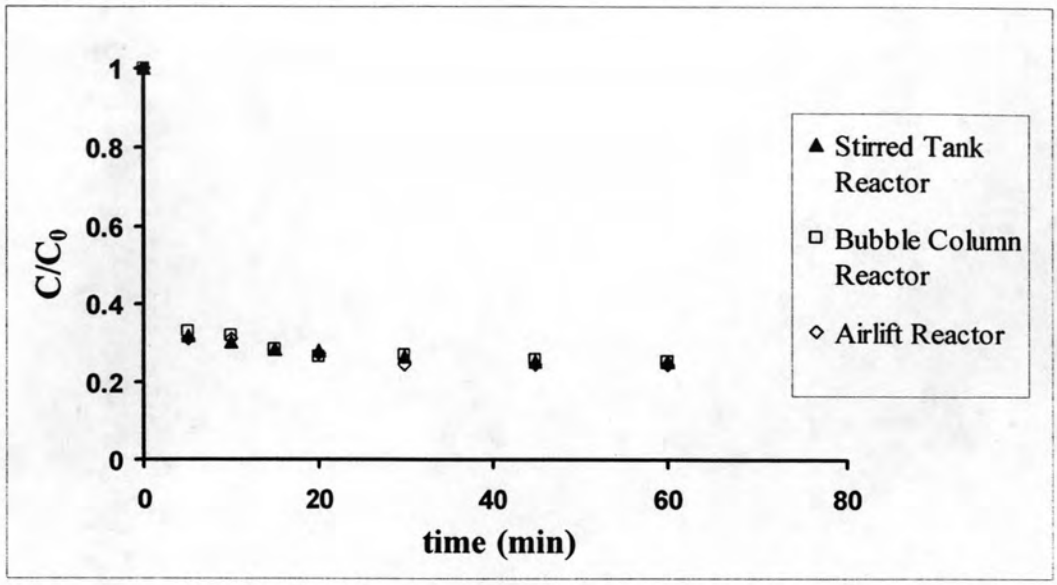

Figure 5.20 Adsorption behavior of crocein orange G on TiO_2 in various types of photoreactors (condition: C_0 = 5 ppm, aeration rate = 12 l/min, pH =2).

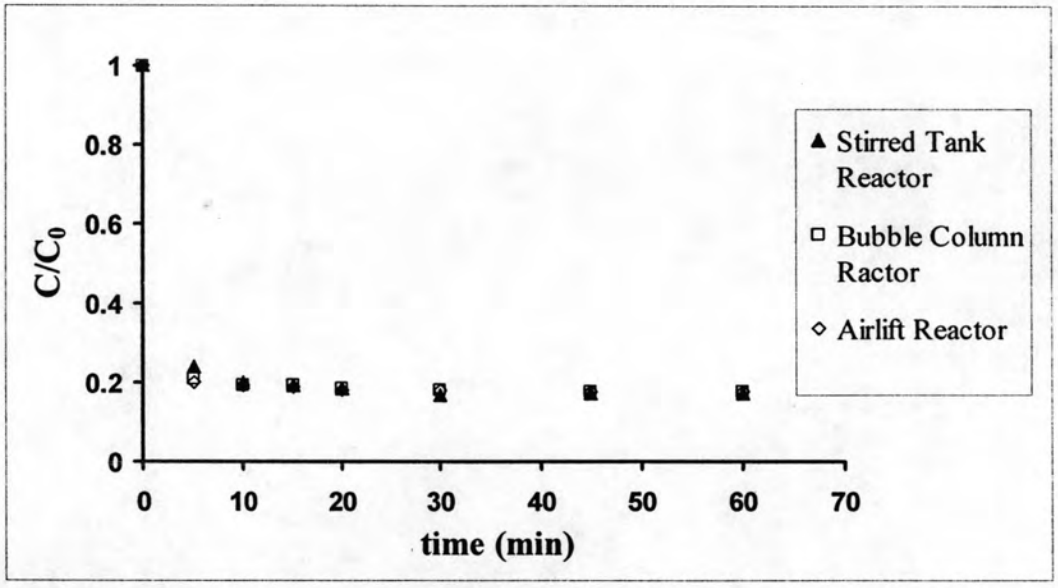

Figure 5.21 Adsorption behavior of crocein orange G on TiO_2 in various types of photoreactors (condition: C_0 = 10 ppm, aeration rate = 12 l/min, pH =2).

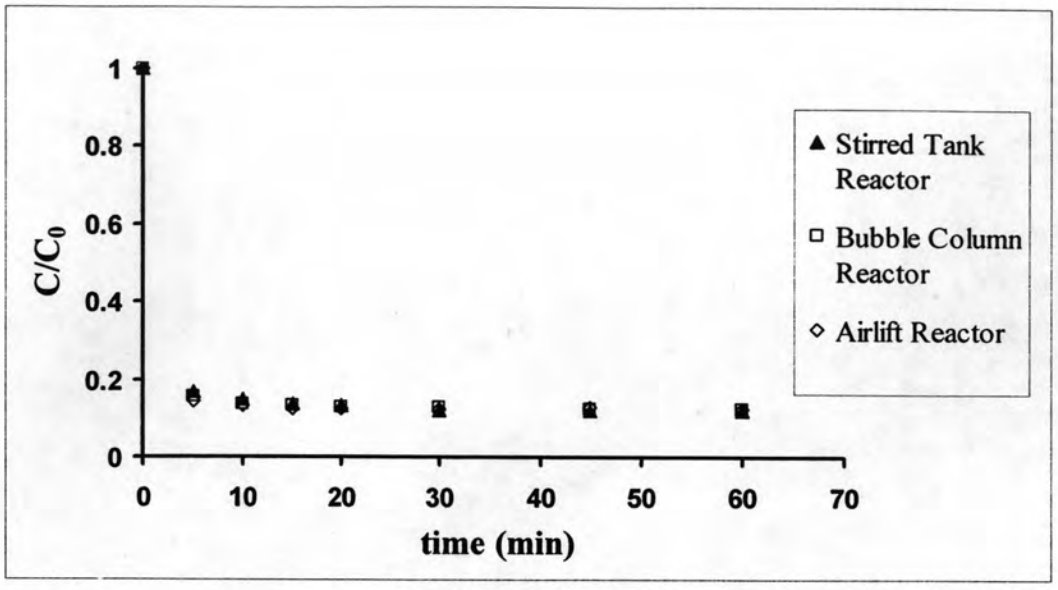

Figure 5.22 Adsorption behavior of crocein orange G on TiO_2 in various types of photoreactors (condition: C_0 = 15 ppm, aeration rate = 12 l/min, pH =2).

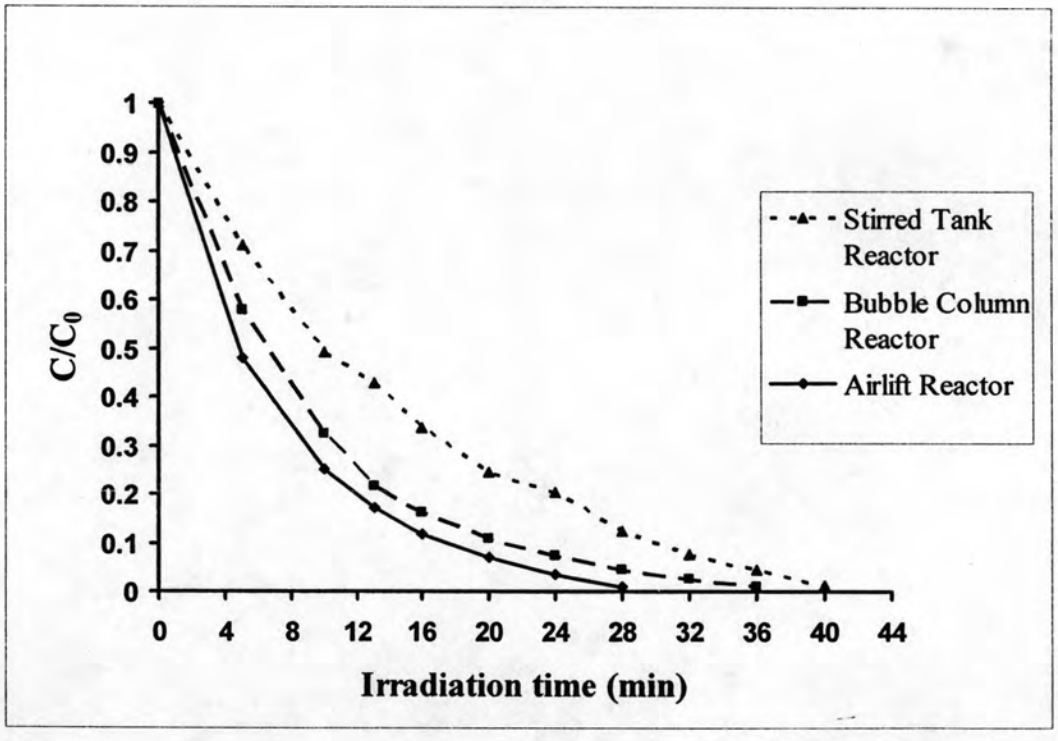

Figure 5.23 Photocatalytic degradation of crocein orange G in various types of photoreactors (condition: C_0 = 5 ppm, aeration rate = 12 l/min, pH =2).

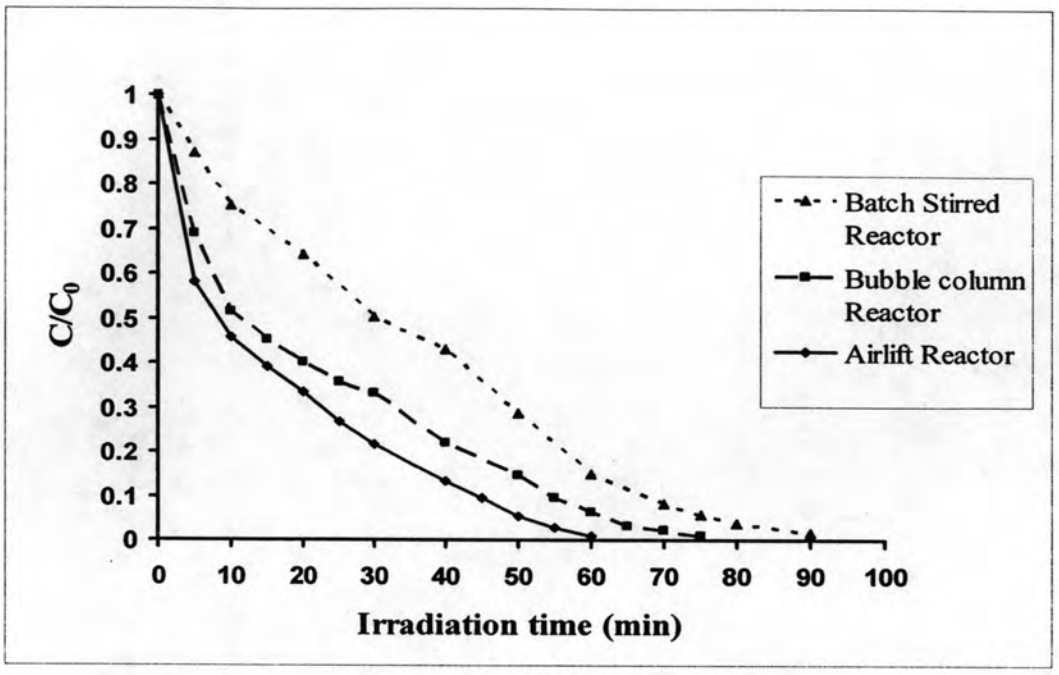

Figure 5.24 Photocatalytic degradation of crocein orange G in various types of photoreactors (condition: C_0 = 10 ppm, aeration rate = 12 l/min, pH =2).

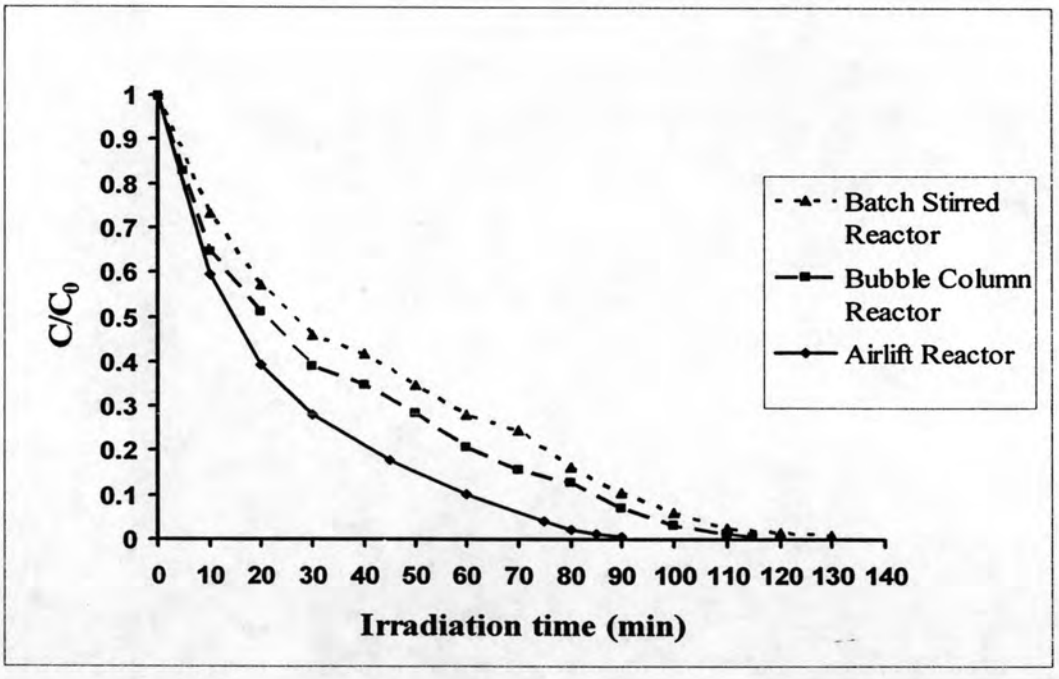

Figure 5.25 Photocatalytic degradation of crocein orange G in various types of photoreactors (condition: C_0 = 15 ppm, aeration rate = 12 l/min, pH =2).

5.2.5.2 Photocatalytic degradation of methylene blue in various reactor systems

Figures 5.26 to 5.28 display the adsorption behavior of methylene blue in three different photoreactor systems at initial concentrations of 5, 10, and 15 ppm, respectively. Different photoreactor systems appeared to have similar adsorption behavior at all values of initial concentration of dye. However, an increase in the initial concentration raised the amount of methylene blue adsorbed on TiO_2

After 60 minutes of adsorption without UV irradiation, the photocatalytic degradation of methylene blue were continuously monitored. Figures 5.29 to 5.31 display the photocatalytic degradation of methylene blue in the three photoreactor systems at various initial concentrations. Among the three photoreactor systems, airlift reactor system still exhibited the best performance in the photocatalytic degradation of the dye at all initial concentrations. With an airlift reactor system, the photocatalytic degradation of methylene blue at initial concentrations of 5, 10, and 15 ppm reached completion in 30 min, 70 min, and 100 min, respectively.

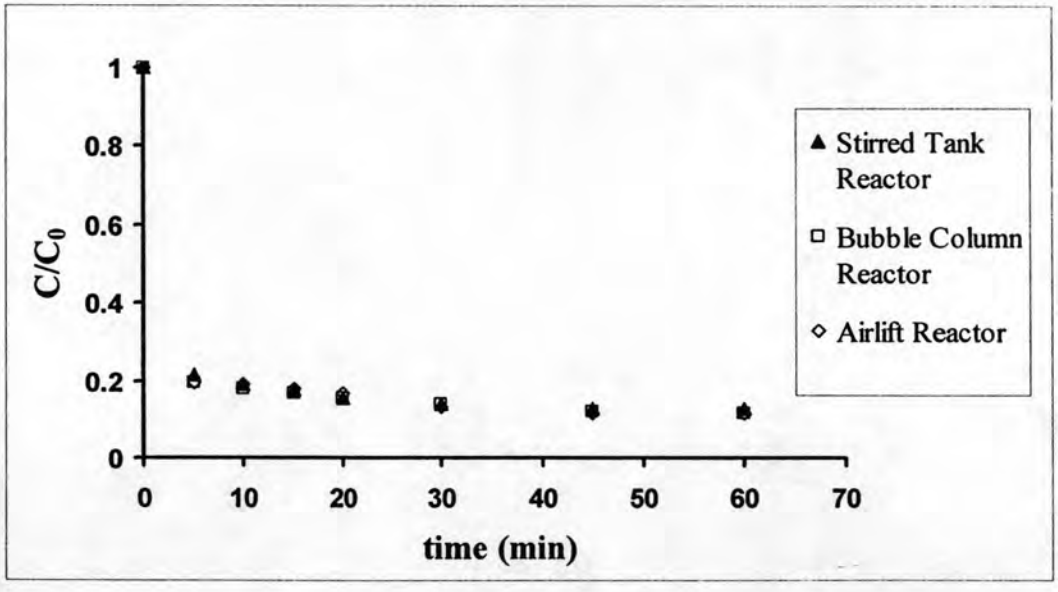

Figure 5.26 Adsorption behavior of methylene blue on TiO_2 in various types of photoreactors (condition: C_0 = 5 ppm, aeration rate = 12 l/min, pH =10).

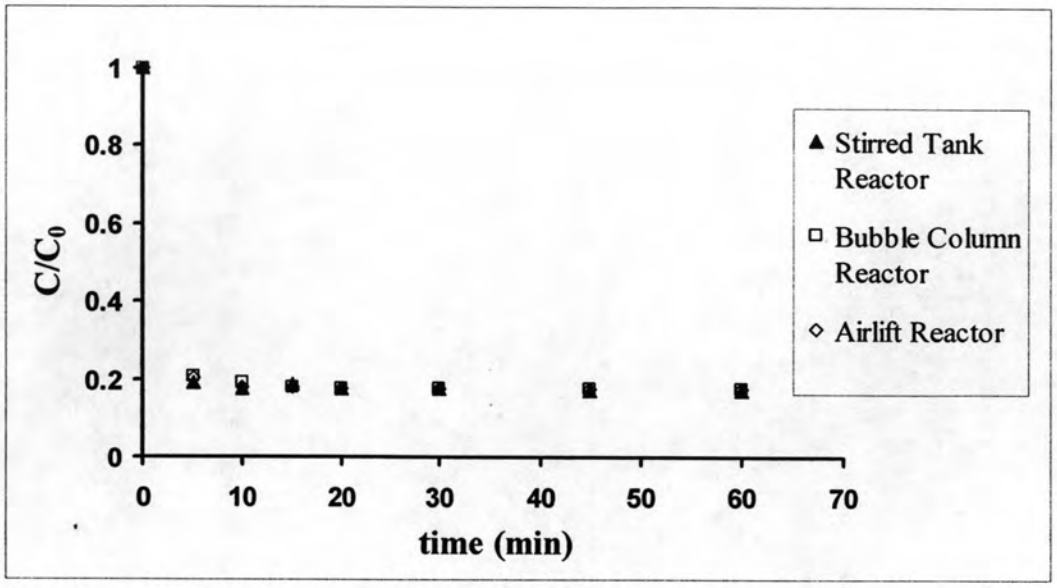

Figure 5.27 Adsorption behavior of methylene blue on TiO_2 in various types of photoreactors (condition: C_0 = 10 ppm, aeration rate = 12 l/min, pH =10).

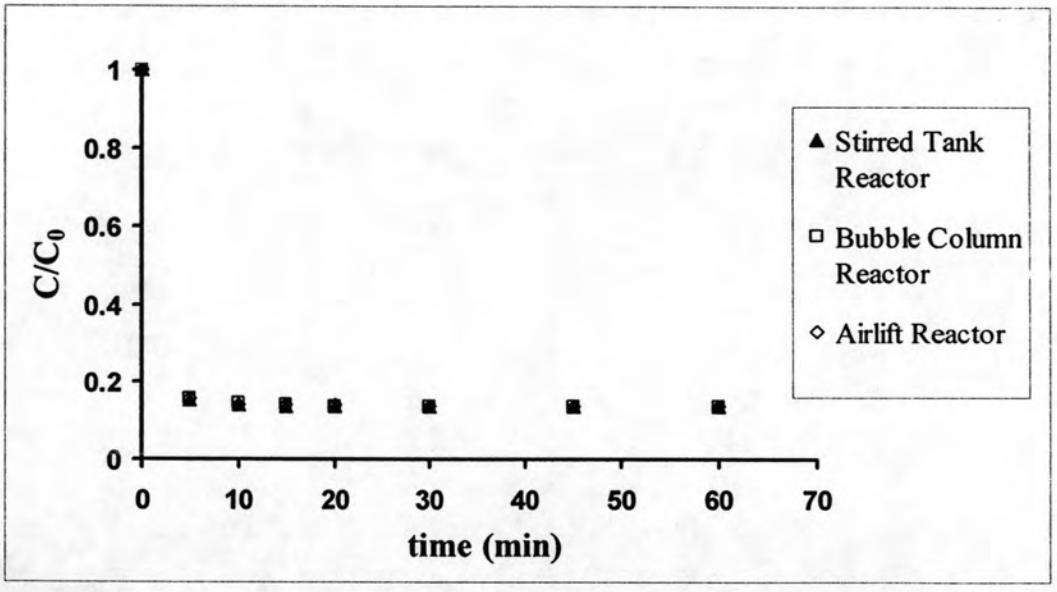

Figure 5.28 Adsorption behavior of methylene blue on TiO_2 in various types of photoreactors (condition: C_0 = 15 ppm, aeration rate = 12 l/min, pH =10).

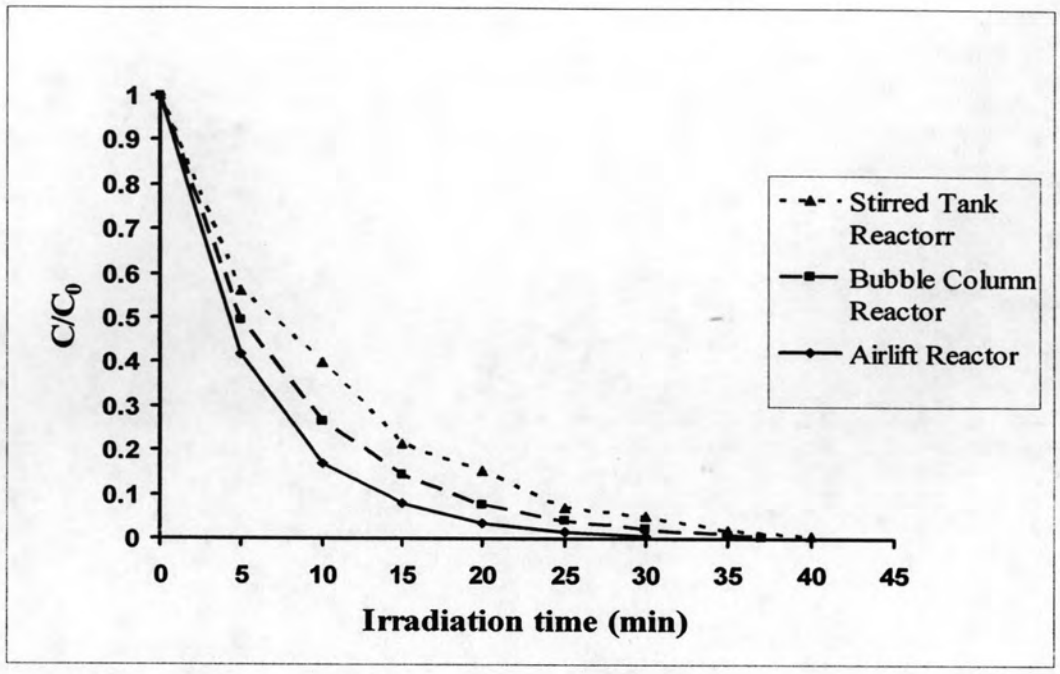

Figure 5.29 Photocatalytic degradation of methylene blue in various types of photoreactors (condition: C_0 = 5 ppm, aeration rate = 12 l/min, pH =10).

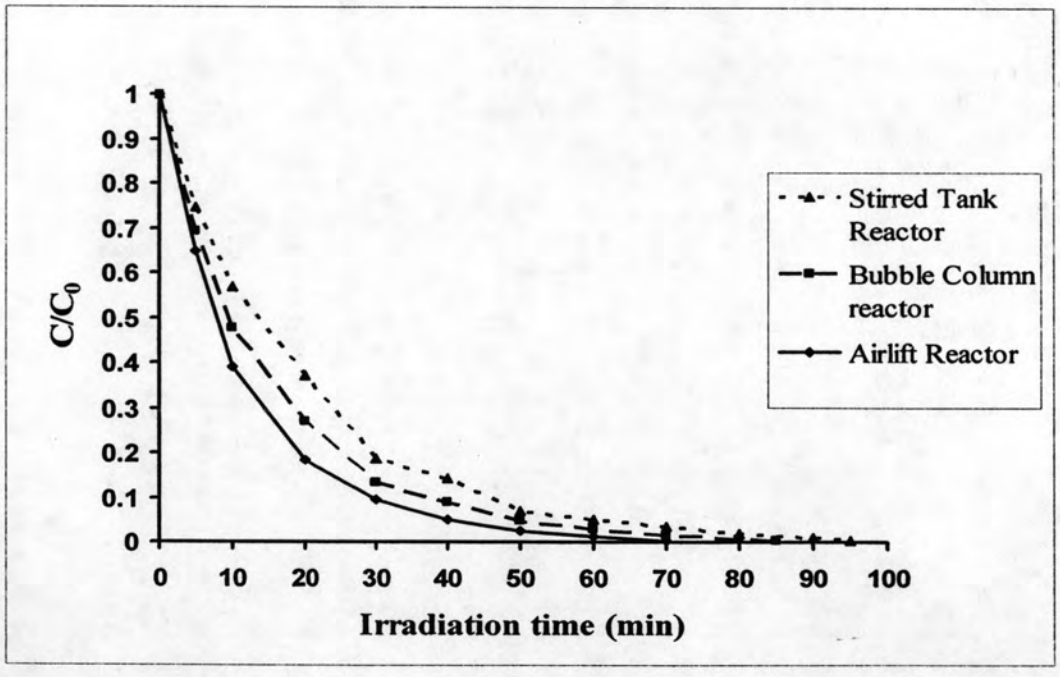

Figure 5.30 Photocatalytic degradation of methylene blue in various types of photoreactors (condition: C_0 = 10 ppm, aeration rate = 12 l/min, pH =10).

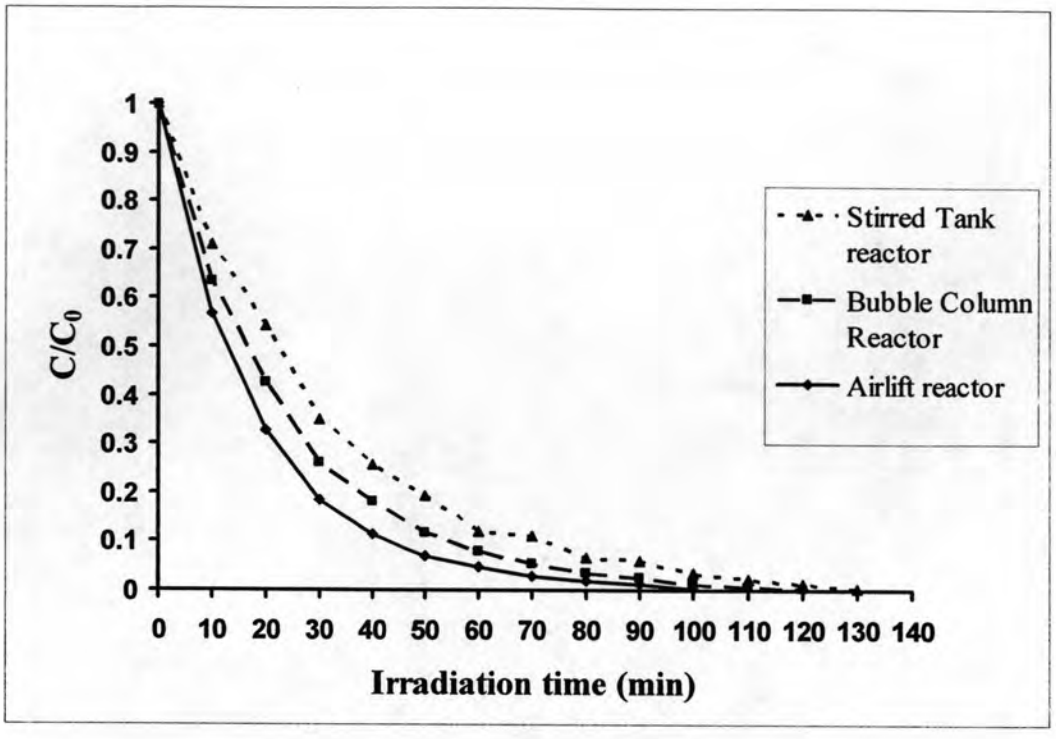

Figure 5.31 Photocatalytic degradation of methylene blue in various types of photoreactors (condition: C_0 = 15 ppm, aeration rate = 12 l/min, pH =10).

To further investigate why an airlift reactor had the best performance for the photocatalytic degradation of dye, dissolved oxygen concentration (DOC) and light intensity inside the reactor were measured during the photocatalytic degradation experiments, for which the initial concentration of dye was 10 ppm.

Figures 5.32 and 5.33 show the dissolved oxygen concentration (DOC) during photocalatytic degradation of crocein orange G and methylene blue, respectively. Figures 5.34 and 5.35 display the light intensity inside the photoreactor during the photocatalytic degradation of crocein orange G and methylene blue, respectively. From Figures 5.32 and 5.33, the DOC in an airlift reactor was essentially the same as the DOC in a bubble column reactor. The DOC's in those two types of photoreactors were significantly higher than that in a stirred tank reactor.

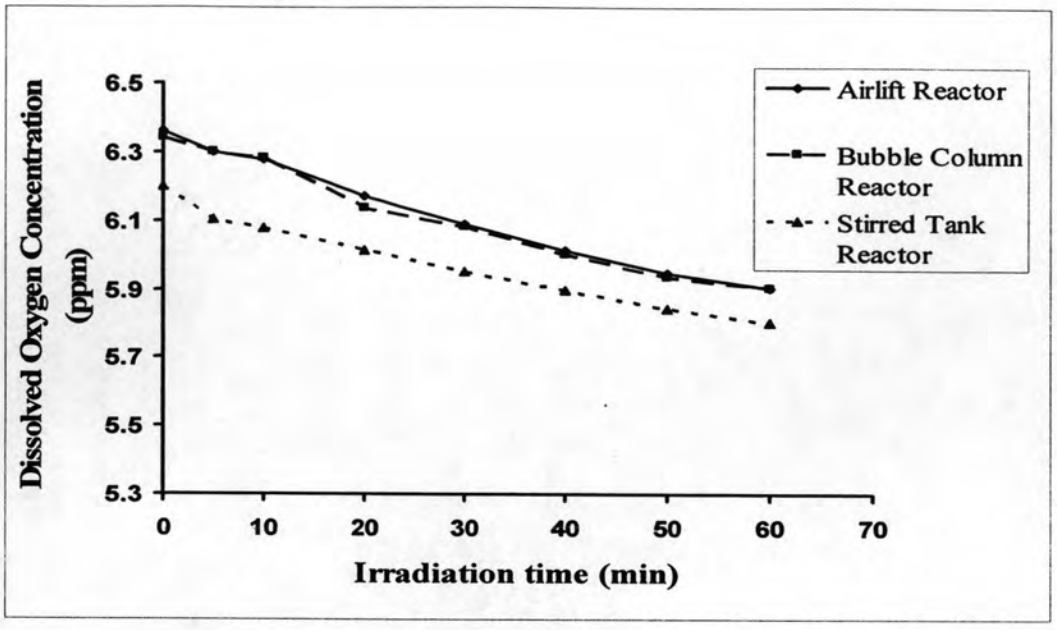

Figure 5.32 Dissolved oxygen concentration during the photocatalytic degradation of crocein orange G in three types of photoreactors (condition: C_0 = 10 ppm, aeration rate = 12 l/min, pH = 2).

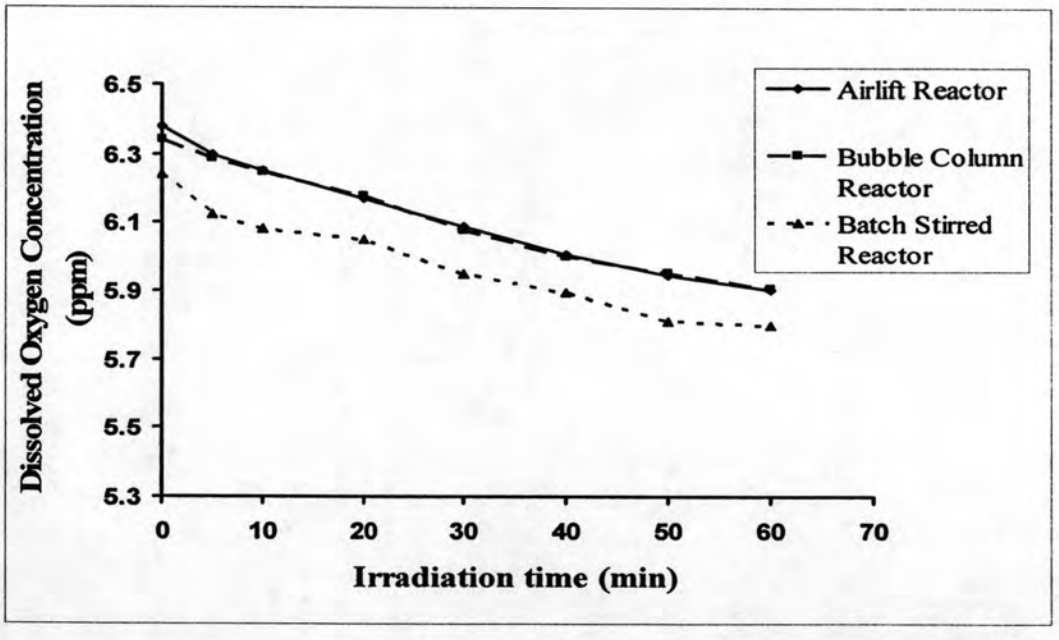

Figure 5.33 Dissolved oxygen concentration during the photocatalytic degradation of methylene blue in three types of photoreactors (condition: C_0 = 10 ppm, aeration rate = 12 l/min, pH = 10).

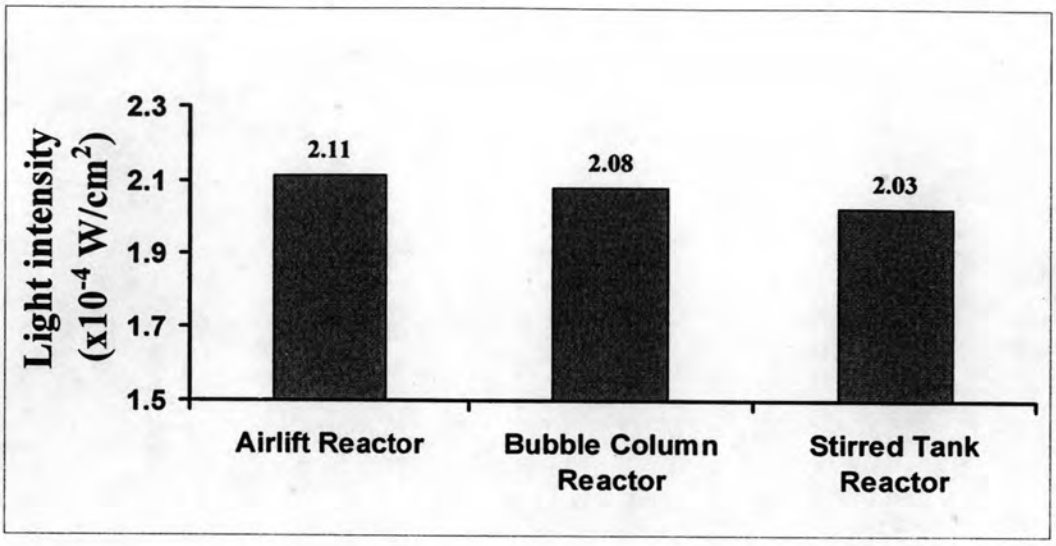

Figure 5.34 Light intensity inside the reactor measured during the photocatalytic degradation of crocein orange G in three types of photoreactors (condition: C_0 = 10 ppm, aeration rate = 12 l/min, pH = 2).

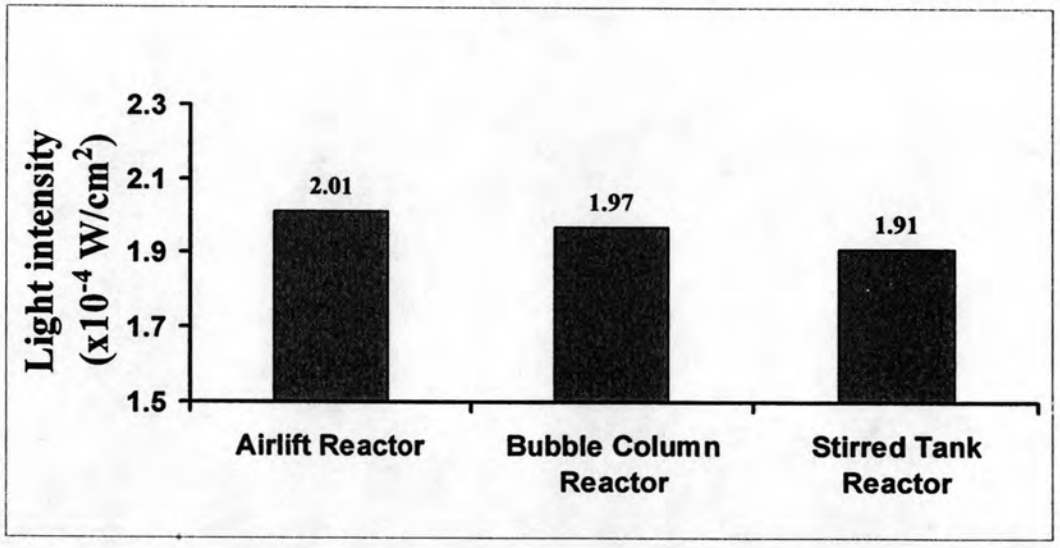

Figure 5.35 Light intensity inside the reactor measured during the photocatalytic degradation of methylene blue in three types of photoreactors (condition: C_0 = 10 ppm, aeration rate = 12 l/min, pH = 10).

Among the three types of photoreactor systems, the light intensity inside the airlift reactor was the greatest while the light intensity inside the stirred tank reactor was the lowest. The small difference in the light intensity between inside the airlift reactor and the bubble column reactor may be a consequence of the larger amount and the wider distribution of air bubbles inside the bubble column reactor, which could hinder the light from getting to the middle of the reactor. The lowest light intensity inside the stirred tank reactor may be attributed to pattern of flow of liquid in the reactor. Liquid inside the stirred tank traveled around the center axis in a circular motion and carried titania along with it. Titania flowing closer to the light source would adsorb most of the light and prevented the light from reaching titania closer to the middle of the beaker. Consideration of both DOC and the light intensity inside the reactor suggest that the stirred tank reactor had the worst performance in photocatalytic degradation of dye.

Between the airlift reactor and the bubble column reactor, there were only small differences in DOC and the light intensity. Therefore, these factors were not the reasons for the better performance in the airlift reactor. The main difference between the airlift reactor system and the bubble column system lie in the fluid flow, which depended on the geometry of the systems. Random mixing in the bubble column reactor was brought about by ascending bubbles. In the airlift reactor system, on the other hand, there was a circulation of fluid in a pattern due to the existence of the draft tube, which did not occur in the bubble column reactor [Merchuk, 1990]. Figures 5.36 and 5.37 display the photographs taken at the bottom of the bubble column reactor and the airlift reactor while the reaction was undergoing, respectively. Figure 5.36 suggest that the mixing in the bubble column reactor was not sufficient as some titania powders could be observed at the bottom of the bubble column reactor. On the other hand, no titania powders was observed at the bottom of the airlift reactor. Good mixing in the airlift reactor gave rise to the better performance for photocatalytic degradation of dye.

Figure 5.36 Image of the bottom of the bubble column reactor during experiment

Figure 5.37 Image of the bottom of the airlift reactor during experiment

5.2.6 Kinetic modeling of the photocatalytic degradation of organic dyes

In this research, the kinetic data from the experiments were fitted by using nonlinear regression analyses. Athena Visual Studio was employed to solve the rate constant. The Langmuir–Hinshelwood model (Eq. (5.4)) was chosen as a model of interest.

$$r = \frac{-dC}{dt} = \frac{k_{app} C}{1 + K_A C} \qquad (5.4)$$

Where r was the photocatalytic degradation rate (mmol L^{-1} min^{-1}), C was the concentration of dye (mmol L^{-1}), k was the apparent reaction rate constant (mmol L^{-1} min^{-1}), and K_A was the adsorption equilibrium constant (L $mmol^{-1}$).

Linearization of the nonlinear model was employed to determine the initial estimates of the nonlinear parameters (k and K_A) because nonlinear regression analysis required good initial estimates for the parameters in the model

The results for apparent reaction rate constant k_{app} as estimated by Athena Visual Studio were listed into two tables. Table 5.1 and 5.2 shows the apparent reaction rate constants for all experiments involving photocatalytic degradation of crocein orange G and methylene blue respectively. Kinetic data and the best fit curves determined from nonlinear regression analyses for all experiments and displayed in Figures 5.38 to 5.48

Estimates of the apparent reaction rate constant obtained from nonlinear regression analyses were in excellent agreement with the experimental results when effects of various parameters were discussed in previous sections. For example:

- k_{app} increased as aeration rate increased
- k_{app} decreased as initial concentration of dye increased
- the airlift reactor had the highest k_{app}
- k_{app} was the highest for crocein orange G and methylene blue when pH was 2 and 10, respectively

Table 5.1 Estimates of the apparent reaction rate constants obtained from nonlinear regression analyses at various conditions for the photocatalytic degradation of crocein orange G.

Effect of aeration rate	
Crocein orange G, C_0 = 5 ppm, pH = 5.57	k_{app} (min^{-1})
Aeration rate =12 l/min	0.036269
Aeration rate = 9 l/min	0.031480
Aeration rate = 6 l/min	0.022315
Effect of initial concentration	
Crocein orange G, pH = 5.57, aeration rate = 12 l/min	k_{app} (min^{-1})
C_0 = 5 ppm	0.036269
C_0 = 10 ppm	0.016080
C_0 = 15 ppm	0.012649
Effect of pH	
Crocein orange G, C_0 = 5 ppm aeration rate = 12 l/min	k_{app} (min^{-1})
pH = 2	0.135214
pH = 4	0.056506
pH = 5.57	0.036269
pH = 8	0.010825
Effect of types of photoreactors	
Crocein orange G, C_0 = 5 ppm, pH = 2, aeration rate = 12 l/min	k_{app} (min^{-1})
Airlift reactor	0.135214
Bubble column reactor	0.109880
Stirred tank reactor	0.082101
Crocein orange G, C_0 = 10 ppm, pH = 2, aeration rate = 12 l/min	k_{app} (min^{-1})
Airlift reactor	0.059270
Bubble column reactor	0.045170
Stirred tank reactor	0.030946
Crocein orange G, C_0 = 15 ppm, pH = 2, aeration rate = 12 l/min	k_{app} (min^{-1})
Airlift reactor	0.043775
Bubble column reactor	0.028865
Stirred tank reactor	0.020360

Table 5.2 Estimates of the apparent reaction rate constants obtained from nonlinear regression analyses at various conditions for the photocatalytic degradation of methylene blue.

Effect of initial concentration	
Methylene blue, pH = 5.37, aeration rate = 12 l/min	k_{app} (min^{-1})
C_0 = 5 ppm	0.094373
C_0 = 10 ppm	0.050047
C_0 = 15 ppm	0.027546
Effect of pH	
Methylene blue, C_0 = 5 ppm, aeration rate = 12 l/min	k_{app} (min^{-1})
pH = 4	0.061292
pH = 5.37	0.119111
pH = 8	0.121955
pH = 10	0.189664
Effect of types of photoreactors	
Methylene blue, C_0 = 5 ppm, pH = 10, aeration rate = 12 l/min	k_{app} (min^{-1})
Airlift reactor	0.189664
Bubble column reactor	0.145876
Stirred tank reactor	0.133654
Methylene blue, C_0 = 10 ppm, pH = 10, aeration rate = 12 l/min	k_{app} (min^{-1})
Airlift reactor	0.085700
Bubble column reactor	0.067172
Stirred tank reactor	0.052655
Methylene blue, C_0 = 15 ppm, pH = 10, aeration rate = 12 l/min	k_{app} (min^{-1})
Airlift reactor	0.055388
Bubble column reactor	0.043435
Stirred tank reactor	0.033256

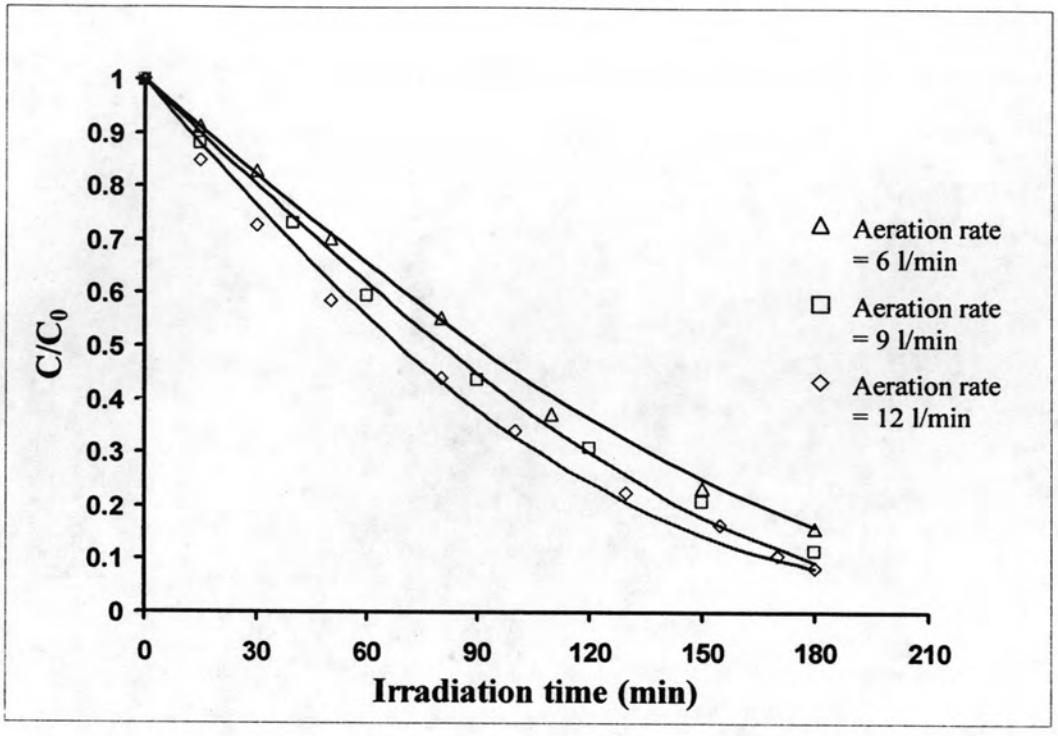

Figure 5.38 Kinetic data for the photocatalytic degradation of crocein orange G at various aeration rates. The lines correspond to the best fit curves as determined from nonlinear regression analysis of the data using a Langmuir–Hinshelwood rate expression.

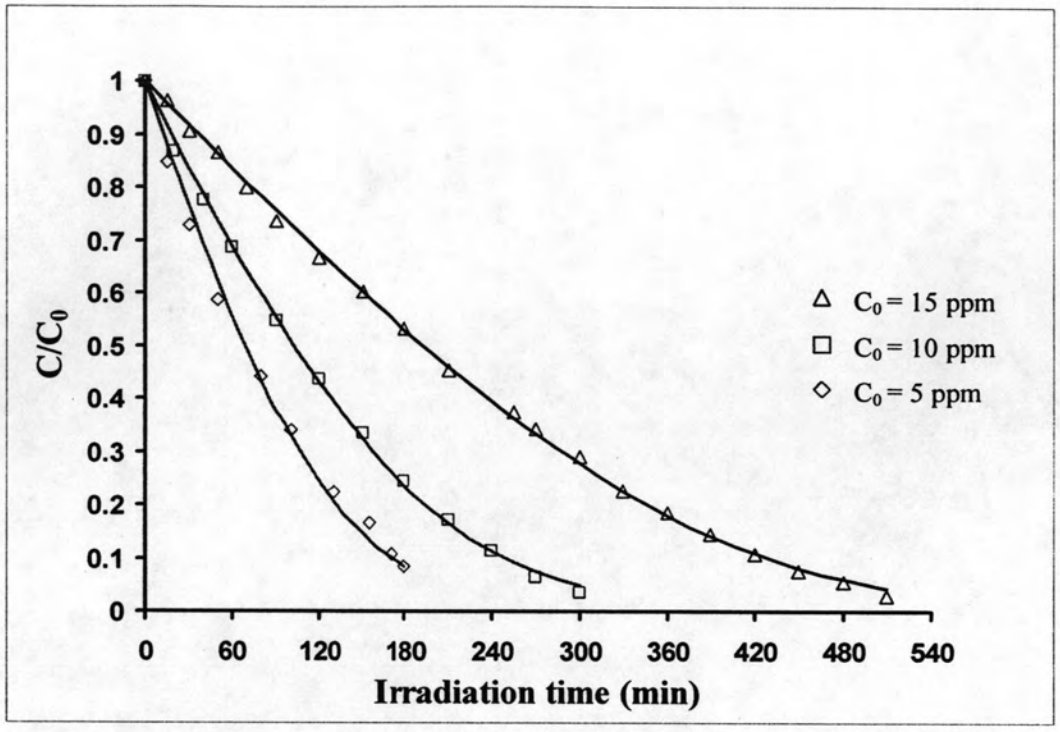

Figure 5.39 Kinetic data for the photocatalytic degradation of crocein orange G at various initial concentrations. The lines correspond to the best fit curves as determined from nonlinear regression analysis of the data using a Langmuir–Hinshelwood rate expression.

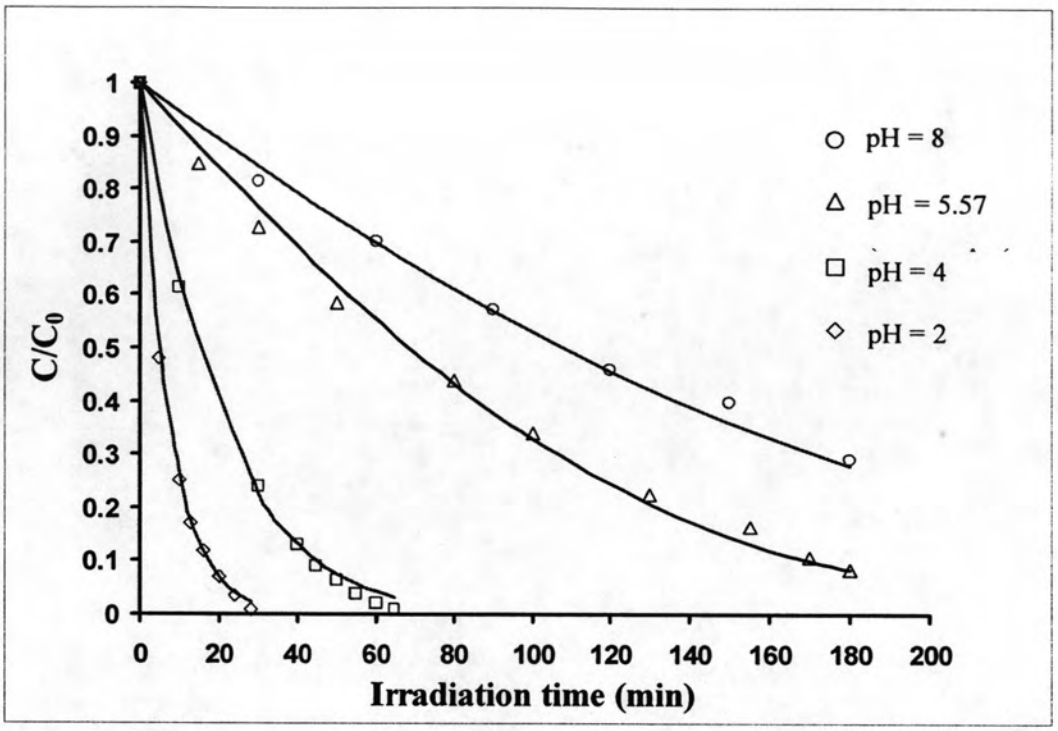

Figure 5.40 Kinetic data for the photocatalytic degradation of crocein orange G at various pH. The lines correspond to the best fit curves as determined from nonlinear regression analysis of the data using a Langmuir–Hinshelwood rate expression.

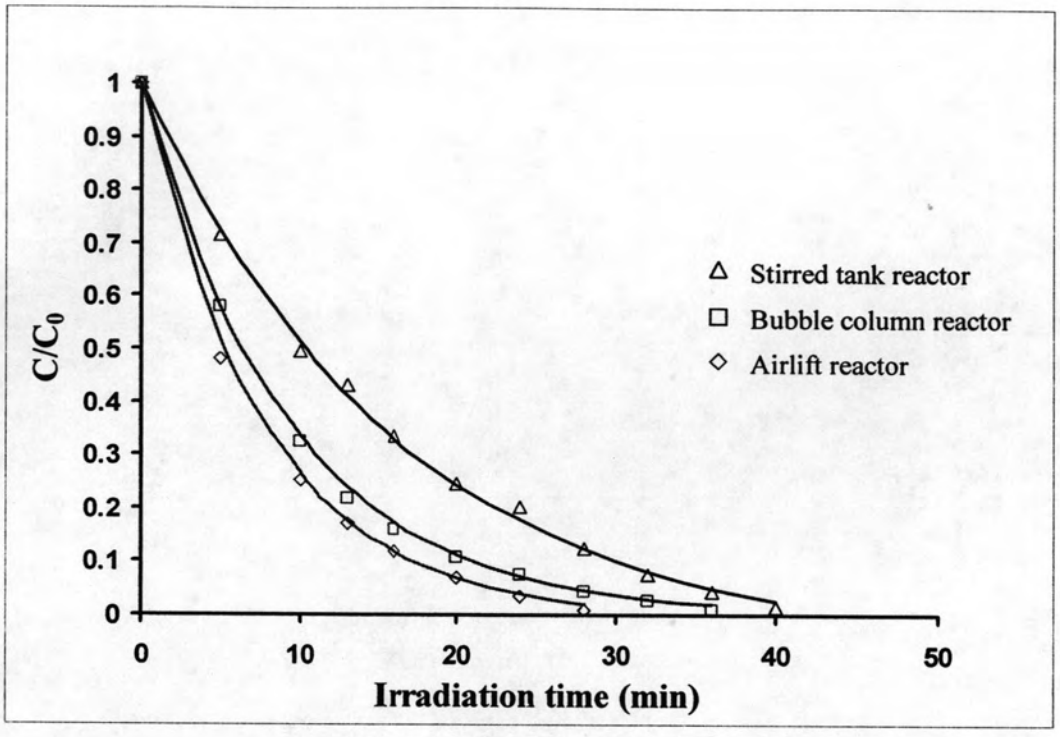

Figure 5.41 Kinetic data for the photocatalytic degradation of 5 ppm crocein orange G at various photoreactor systems. The lines correspond to the best fit curves as determined from nonlinear regression analysis of the data using a Langmuir–Hinshelwood rate expression.

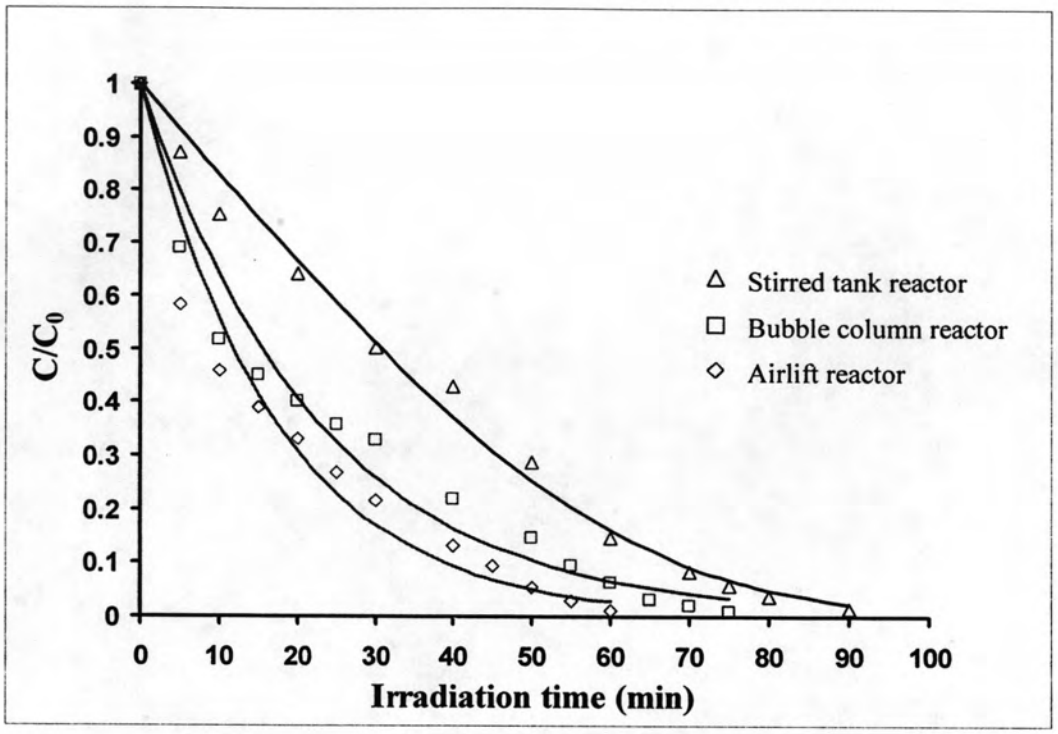

Figure 5.42 Kinetic data for the photocatalytic degradation of 10 ppm crocein orange G at various photoreactor systems. The lines correspond to the best fit curves as determined from nonlinear regression analysis of the data using a Langmuir–Hinshelwood rate expression.

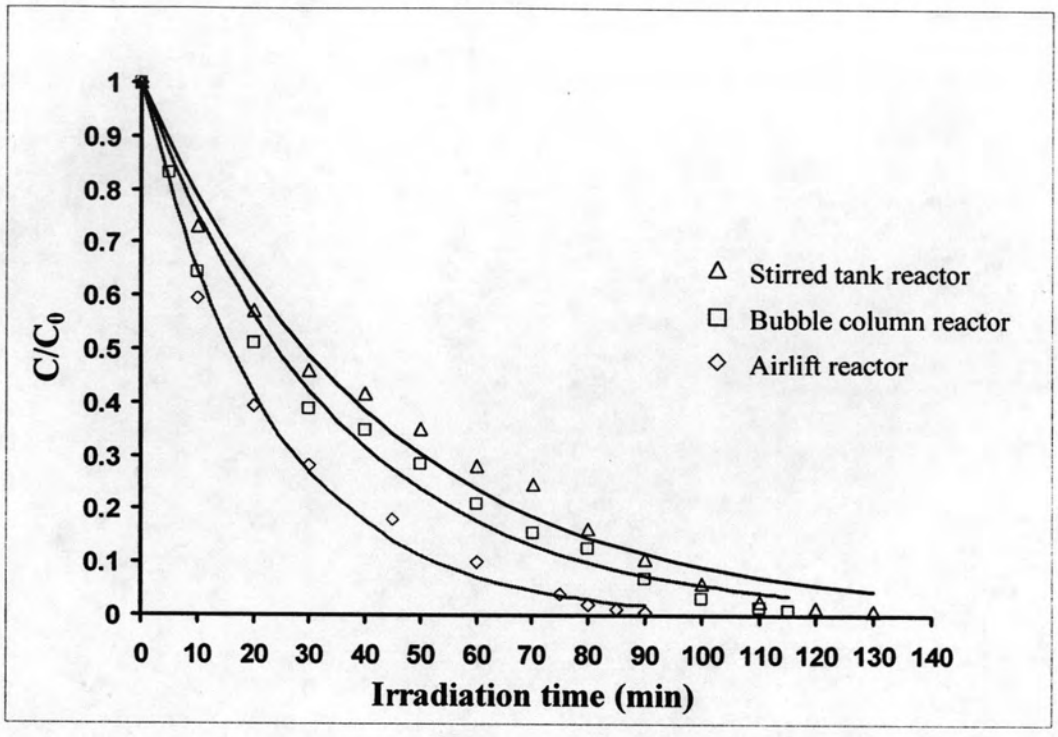

Figure 5.43 Kinetic data for the photocatalytic degradation of 15 ppm crocein orange G at various photoreactor systems. The lines correspond to the best fit curves as determined from nonlinear regression analysis of the data using a Langmuir–Hinshelwood rate expression.

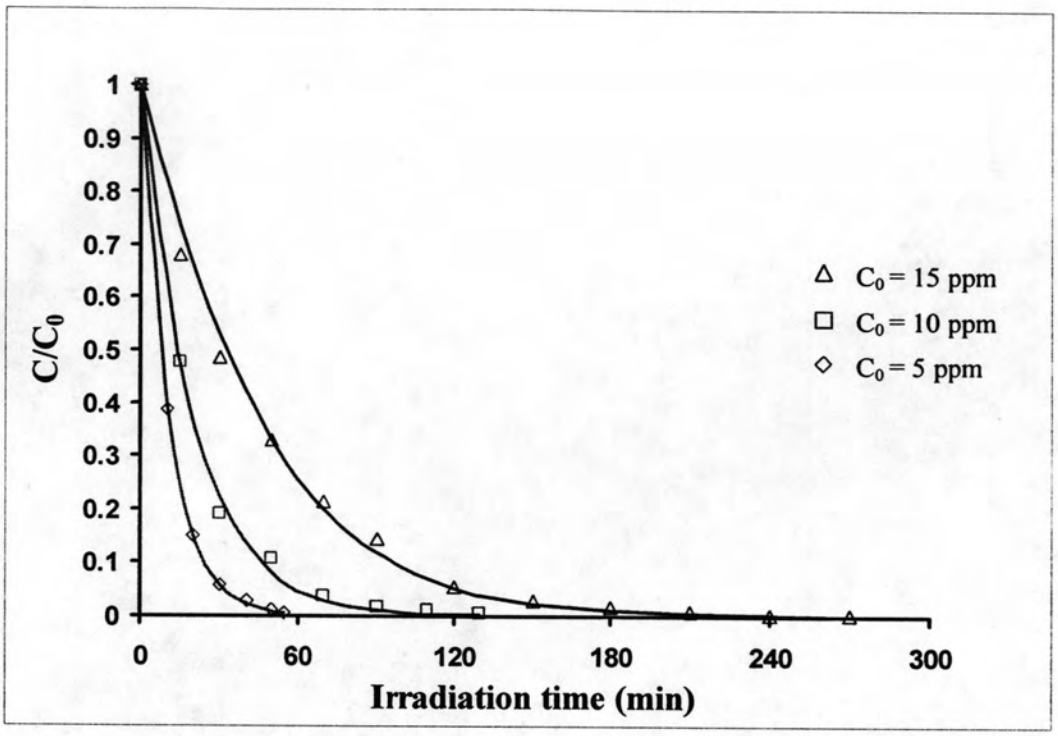

Figure 5.44 Kinetic data for the photocatalytic degradation of methylene blue at various initial concentrations. The lines correspond to the best fit curves as determined from nonlinear regression analysis of the data using a Langmuir–Hinshelwood rate expression.

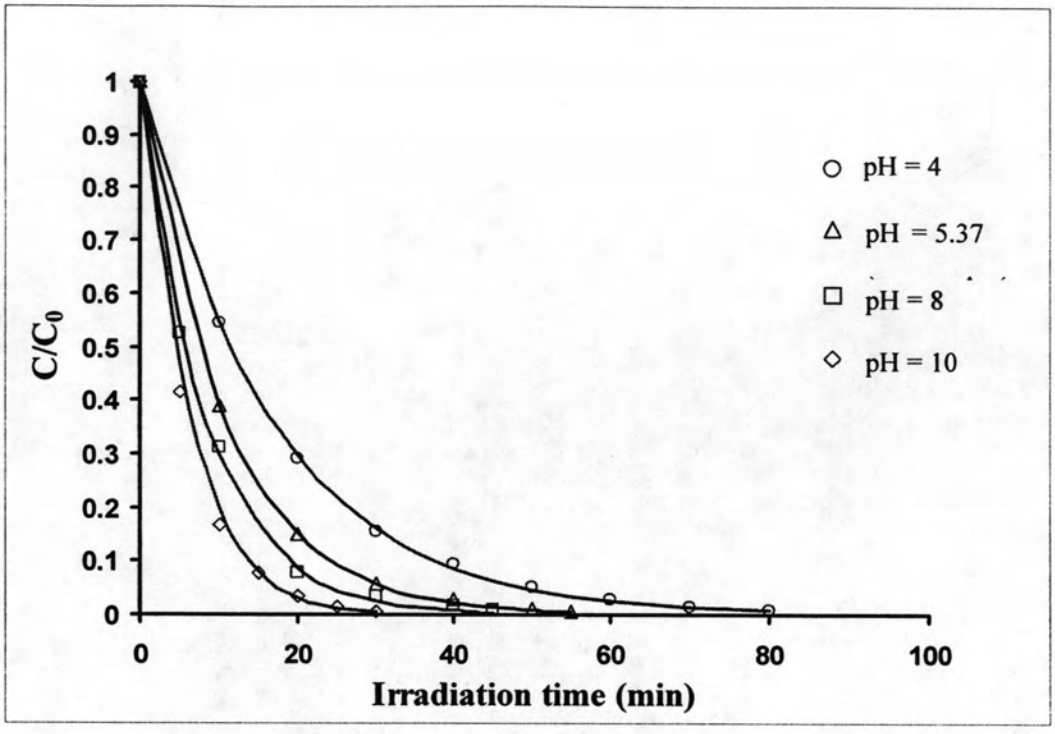

Figure 5.45 Kinetic data for the photocatalytic degradation of methylene blue at various pH. The lines correspond to the best fit curves as determined from nonlinear regression analysis of the data using a Langmuir–Hinshelwood rate expression.

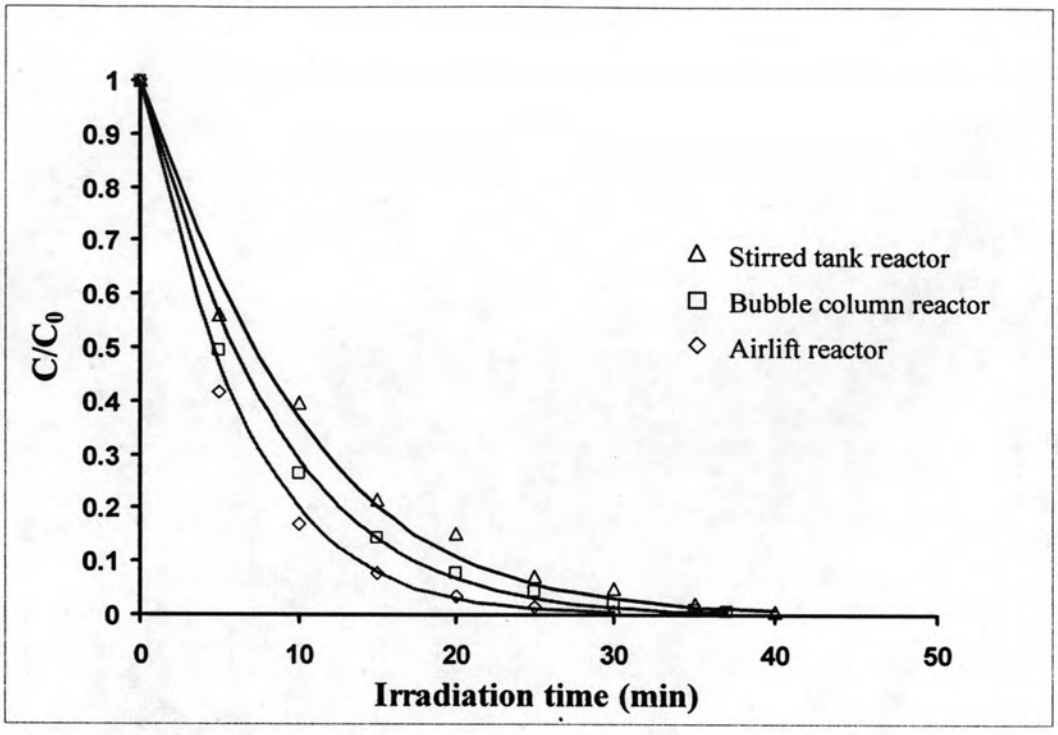

Figure 5.46 Kinetic data for the photocatalytic degradation of 5 ppm methylene blue at various photoreactor systems. The lines correspond to the best fit curves as determined from nonlinear regression analysis of the data using a Langmuir–Hinshelwood rate expression.

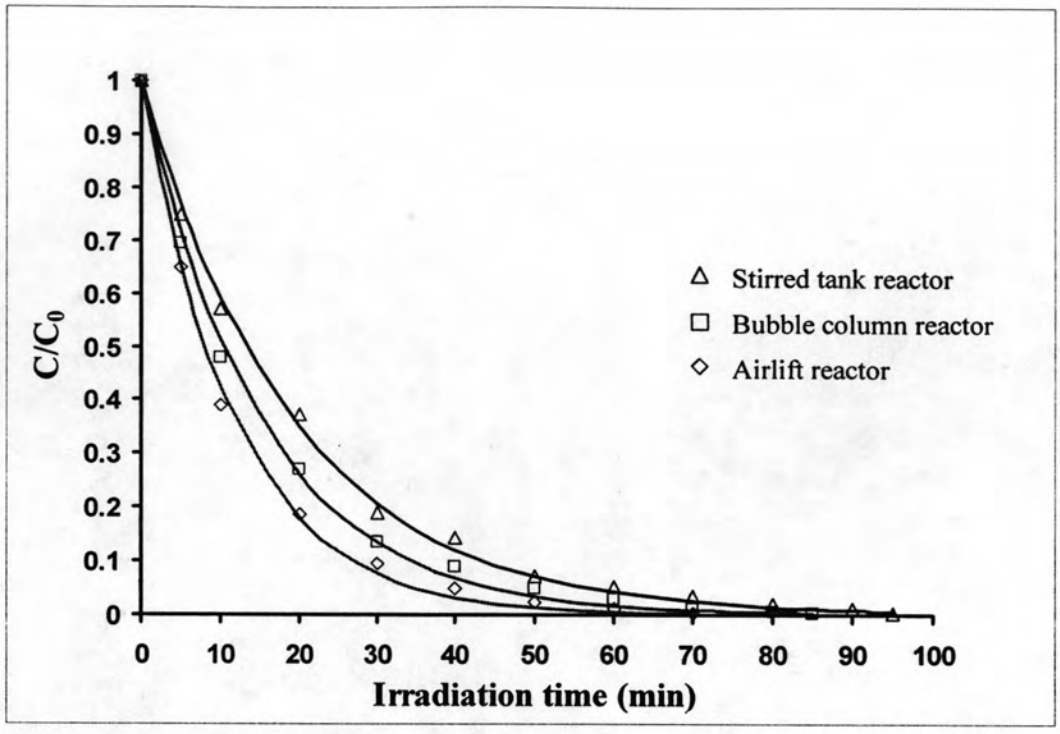

Figure 5.47 Kinetic data for the photocatalytic degradation of 10 ppm methylene blue at various photoreactor systems. The lines correspond to the best fit curves as determined from nonlinear regression analysis of the data using a Langmuir–Hinshelwood rate expression.

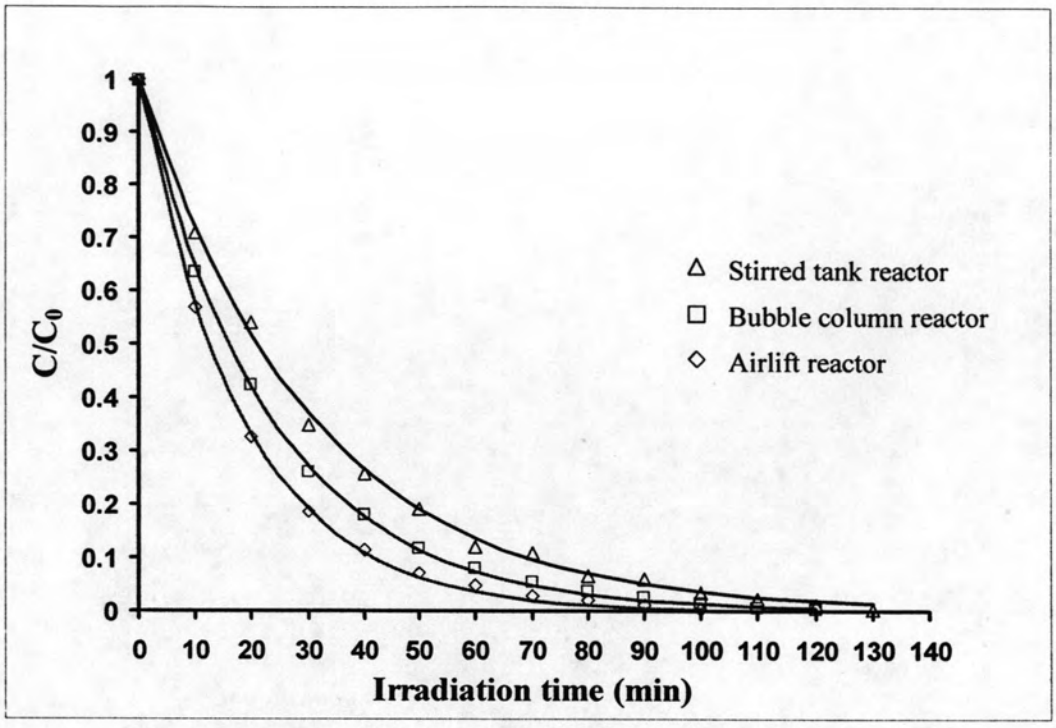

Figure 5.48 Kinetic data for the photocatalytic degradation of 15 ppm methylene blue at various photoreactor systems. The lines correspond to the best fit curves as determined from nonlinear regression analysis of the data using a Langmuir–Hinshelwood rate expression.